UNIVERSITY OF CALIFORNIA, MERCED

Phenotypic and Molecular Characterization of a Human Adult Bone Marrow Committed T Cell Progenitor

THESIS

Submitted in partial satisfaction of the requirements for the degree of

MASTER OF SCIENCE

in Quantitative and Systems Biology

By

Joseph H. Ramos

Thesis committee:

Marcos E. García-Ojeda Ph.D., Chair

Jennifer O. Manilay Ph.D.

David M. Ojcius Ph.D.

Dedicated to

Master Chief Petty Officer Gerardo M. Ramos, U.S. Navy

What is the most resilient parasite? Bacteria? A virus? An intestinal worm? An idea. Resilient. Highly contagious. Once an idea has taken hold of the brain it's almost impossible to eradicate. An idea that is fully formed - fully understood - that sticks; right in there somewhere.

- Cobb from “Inception”

Abstract

Phenotypic and Molecular Characterization of a Human Adult Bone Marrow Committed T Cell Progenitor

Joseph H. Ramos

University of California, Merced, Quantitative and Systems Biology – M.S., 2011

Committee Chair: Marcos E. García-Ojeda Ph.D.

We investigated the phenotypic and molecular characteristics of a rare human adult bone marrow (ABM) $CD34^{+}CD38^{-/lo}CD7^{+}CD10^{-}$ population that comprise 0.04% of the total bone marrow mononuclear cells in search of a human committed T cell progenitor (hCTP). Using multi-color flow cytometry, we investigated our putative hCTP for its cell surface phenotype and sorted cells for molecular analysis. We observed that our putative hCTP population expresses low levels of T cell lineage associated surface markers CD1a and CD5; the chemokine receptors implicated with progenitor migration to the thymus CCR7, CCR9, CXCR6; and lymphoid associated surface markers CD127, CD45RA, and CD24. Using the comparative C_T quantitative PCR method, we established a gene expression profile of our putative hCTP. Molecular analysis reveals that the putative hCTP population lacks expression of T cell lineage genes (*Gata-3*, *CD7*, *CD3ε*) and the lymphoid lineage associated gene *Rag-1*. However, expression of *PU.1* and *Id2* is present in this population, similar to early thymocytes. Based on our results, we conclude that this population resembles the human early thymic progenitor, and is capable of seeding the thymus.

Acknowledgements

First and foremost, I would like to thank my family for the support they have offered. My father embodies the definition of courage and determination, and instilled the work ethic and drive that have helped me achieve my goals in life up to this point. My mother provided a nurturing environment. My sister never ceases to fill me with joy and energy whenever I interact with her.

Next, I would like to thank Nicole Corder. Her perseverance is inspirational to me. Her love, compassion, and patience pushed me forward during the toughest parts of this process. She constantly reminds me to always look at the bright side of life, and to always reach for the stars.

I also want to acknowledge my colleagues at UC Merced: Corey Cain, Heather Thompson, Mufhadal Al-Kuhlani, Harshani Peiris, and Jesús Ciriza. I looked up to you all as scientists. Your encouragement and the friendly environment you created in the workplace did wonders for my sanity.

I would also like to thank my thesis committee for the guidance they have provided throughout my graduate school adventure. To my advisor Dr. Marcos García-Ojeda, your unwavering confidence, training, and support have transformed me from a fledgling undergraduate researcher into an independent thinking scientist. To Dr. Jennifer Manilay and Dr. David Ojcius, I could not have asked either of you for more as committee members.

Finally, I would like to gratefully acknowledge the University of California Cancer Research Coordinating Committee (CRCC) for funding this project.

List of Tables

List of Figures

Page

Table of contents

Chapter 1 - Introduction

1.1 Hematopoietic stem cell transplantation

Hematopoietic stem cell transplantation (HSCT) remains the chief medical procedure for treating hematological diseases and certain types of cancers. These include leukemias, lymphomas, severe aplastic anemia, inherited immune system disorders, and myeloproliferative disorders (1). Ideally, perfectly HLA-matched donors would be used for HSCT due to decreased risk of infections, cytomegalovirus (CMV) reactivation, and mortality due to post-procedure complications (16, 20). However, with nearly 6,000 known HLA Class I and Class II molecules, perfect HLA matches are rare. This necessitates the use of allogeneic HSCT (allo-HSCT). According to the National Marrow Donor Program (NMDP), California transplant centers allow for a maximum of two mismatched HLA loci between donors and recipients. However, allo-HSCT can lead to post-procedure complications. Alloreactive donor T cells contaminating the graft launch an immune response against the host, resulting in graft-versus-host disease (GVHD) (17, 18). Reciprocally, the cells that mediate engraftment and provide the beneficial graft-versus-tumor (GVT) effect are lost if T cells are depleted from the graft (67). Furthermore, since hematopoietic stem cells (HSCs) are slow to reconstitute the T cell compartment post-HSCT, the patient is left immunodeficient for several months (40).

The approach in this project for improving survival after allogeneic HSCT involves the transplantation of T cell progenitors that quickly regenerate the patient's T cell pool and provide the GVT effect, while minimizing the chances of GVHD. A transplantable murine progenitor population committed to the T cell lineage has been

described (23), but the identification of a human equivalent remains to be firmly established.

1.2 The Murine Committed T cell Progenitor

Mouse bone marrow contains a population of $Lin^{-}CD90.2^{+}CD2^{-}$ committed T cell progenitors (CTPs) that swiftly reconstitute T cells in allo-HSCT without inducing GVHD (23). These murine CTPs express *Ptcra*, *Rag-1*, *Rag-2*, and have their *TCR*Vβ loci in germline configuration (43, 41). Furthermore, they exhibit a gene expression profile expected of a T cell progenitor, with *Gata-3*, *TCF-1*, *IL-7R*α, and sterile Cβ transcripts present (23). Studies demonstrated that murine CTPs are capable of generating mature T cells in irradiated wild-type or athymic hosts. These T cells do not induce GVHD when transplanted into allogeneic hosts (23, 41). When challenged with a lethal dose of murine cytomegalovirus (CMV), mice transplanted with 500 mCTPs generated T cells that protect against infection (23). However, the existence of an equivalent population within human bone marrow to the murine committed T cell progenitor has yet to be elucidated.

1.3 Human progenitor populations capable of T cell differentiation

Human bone marrow and cord blood contain hematopoietic stem cells capable of reconstituting T cells *in vitro*. These human hematopoietic stem cells and their progenitor cells have been identified based on the cell surface expression of CD34 (68). It is within the $CD34^{+}$ compartment that much of the search for T cell progenitors has been done, and a number of multipotent progenitors from cord blood and bone marrow have been elucidated based on CD34 surface expression (22, 35, 57, 61, 64). Although the

progenitor populations from each source differ in their capacities to differentiate into a T cell-like phenotype, they set the foundation for this study.

The ability of human adult bone marrow (ABM) and thymus $CD34^+$ populations to both differentiate into T cells when cultured in fetal thymic organ cultures (FTOC) (61) indicates that understanding human early thymocyte development may be beneficial for identifying early T cell progenitors within the bone marrow. Thymic $CD34^+Lin^-$ cells are restricted to the $CD3^-TCR\alpha\beta^-TCR\gamma\delta^-$ compartment (64), and expresses CD7, the earliest T cell lineage marker (22, 64). The $CD34^+CD1a^-$ phenotype was identified as the most immature thymocyte phenotype (64), and the progression through CD4/CD8 double negative phases can be tracked by expression of CD7, CD38, and CD1a (60, 62, 69, summarized in Table 1).

A number of studies have further established the importance of CD7 for identifying T cell progenitors in the human bone marrow (summarized in Table 2): One study demonstrated that *in vitro* colonization of thymic lobes by adult bone marrow $CD34^+Lin^-$ is enhanced by the surface expression of CD7 (61). Although $CD34^+CD7^+Lin^-$ cells from the adult human bone marrow retain the capability to differentiate into granulocytes and monocytes in long-term marrow culture (60, 63), this population on average produces 20 times fewer myeloid colonies than the $CD34^+CD7^-$ compartment (63). Terstappen et al. reported a fetal bone marrow (fetal BM) $CD34^+CD7^+CD5^+CD2^+$ population that exhibited a cell surface phenotype similar to early thymocytes (64). However, their study did not examine for T cell potential using differentiation assays, and observed that this population is absent in ABM. Haddad et al. identified a $CD34^{hi}Lin^-CD45RA^{hi}CD7^+$ fetal BM population that emerges by 8-9 weeks

of development, and possesses NK and T cell, but limited B cell, differentiation potential (22). These cells expressed low levels of CD38, CD2, CXCR4, and CCR9, but lacked CD5 surface expression. Furthermore, this phenotype declines around birth. An *in vitro* study by Rossi et al. (34) examined the differentiation of ABM $CD34^{+}CD7^{+}CD10^{-}Lin^{-}$ and $CD34^{+}CD7^{-}CD10^{+}Lin^{-}$ cells on MS5 stromal cells. Their experiments revealed that compared to the $CD7^{-}CD10^{-}$ and $CD7^{-}CD10^{+}$ ABM populations, the $CD7^{+}CD10^{-}$ subset transiently produced NK cells after 3 weeks of culture, but did not differentiate into $CD19^{+}$ B cells after 5 weeks of culture. Given the notion that T and NK cell differentiation are more developmentally related (56), the data from Rossi et al. suggests that the $CD7^{+}CD10^{-}$ ABM population may be skewed toward the T cell lineage.

In vitro differentiation experiments using $CD34^{+}CD38^{-/lo}$ human hematopoietic stem cells (hHSCs) from various donor sources have also been used to study T cell differentiation (7, 22, 47, 30). When co-cultured on OP9-delta-like-1 (OP9-DL1) stroma, umbilical cord blood (UCB) $CD34^{+}CD38^{-/lo}$ populations exhibited early steps of T cell differentiation (7). These progenitors rapidly gained expression of CD7 as quickly as 4 days after co-culture, CD5 expression by day 8 of culture, and CD1a by day 10 of culture. This study also revealed that the $CD34^{+}CD38^{-/lo}Lin^{-}$ fraction possessed a 5-fold increase in T lymphoid progenitor frequency on OP9-DL1 culture when compared to the $CD34^{+}CD38^{+/hi}Lin^{-}$ subset (7). In two separate studies, Smedt et al. co-cultured ABM hHSCs with OP9-DL stromal cells, which generated $CD4^{+}CD8^{+}CD3^{+}$ T cells after 35 days, and $TCR\alpha\beta^{+}$ cells by day 44 (30, 2). ABM hHSCs progressed through $CD5^{+}CD7^{+}CD1^{-}CD4^{-}$ and $CD5^{+}CD7^{+}CD1^{-}CD4^{+}$ early T cell progenitor phenotypes on OP9-DL1 (30). The $CD34^{+}CD38^{+/hi}CD5^{+}CD7^{+}CD4^{-}CD1a^{-}Lin^{-}$ generated after 35 days of

ABM culture proceeded to generate a low percentage of $CD4^+$ single positive (SP), $CD4^+CD8^+$ double positive (DP), $TCR\alpha\beta^-CD3^+$, and $TCR\alpha\beta^+CD3^+$ cells by day 49 (2). Moreover, the frequency of generating $CD14^-CD15^+$ granulocytes and $CD14^+HLA\text{-}DR^+$ monocytes after 21 days in OP9 culture was shown to be comparable between the two sources, suggesting that the slower progression in T cell differentiation is not due increased myeloid potential by ABM hHSCs.

Combining the information in literature regarding the surface markers used for identification of T cell precursors, we hypothesize that the $CD34^+CD38^{-/lo}CD7^+CD10^-Lin^-$ ABM population is the human committed T cell progenitor (hCTP). However, cell surface phenotype alone cannot establish the existence of the hCTP. Therefore, molecular analysis to determine gene expression profile is needed.

Table 1 – Comparison between human and murine double negative (DN) thymocyte stages.

DN stage	**Organism**	
	Murine	**Human**[60, 69]
DN1	$CD44^{+}CD25^{-}$	$CD34^{+}CD7^{+}CD38^{-}CD1a^{-}$
DN2	$CD44^{+}CD25^{+}$	$CD34^{+}CD7^{+}CD38^{+}CD1a^{-}$
DN3	$CD44^{-}CD25^{+}$	$CD34^{+}CD7^{+}CD38^{+}CD1a^{+}$
DN4	$CD44^{-}CD25^{-}$	?

Table 2 – Summary of human candidate bone marrow T cell progenitors.

Stage of development	**Phenotype**	**Lineage potential**	**Culture conditions**	**Presence in ABM**
Fetal[64]	$CD34^{+}CD7^{+}CD5^{+}CD2^{+}$	Not determined	Not cultured	Not detected
Fetal up to birth[22]	$CD34^{hi}CD7^{+}CD45RA^{hi}$	2 weeks: NK cell, limited B. 4 weeks: DP T cell	MS5 stroma + Flt-3L, IL-2, IL-7, IL-15 (NK cell) MS5 stroma + IL-7 (B cell) FTOC for T cell	Declines after birth
Post-natal/ Adult[34]	$CD34^{+}CD7^{+}CD10^{-}Lin^{-}$	3 weeks: NK, no B, decreased myeloid	MS5 stroma + SCF, G-CSF, Flt-3L, IL-15 (multi-lineage condition)	Present
Post-natal/ Adult[61]	$CD34^{+}CD7^{+}Lin^{-}$	DP ($CD4^{+}CD8^{+}$), SP (CD4+/CD8+) T cells	FTOC	Present

1.4 Molecular characteristics of progenitors capable of T cell differentiation

To our knowledge, no evidence exists describing the molecular characteristics of ABM $CD34^{+}CD38^{-/lo}CD7^{+}CD10^{-}Lin^{-}$ cells. However, several studies have probed progenitor populations with similar cell surface phenotypes for their gene expression profiles and arrangement status of the T cell receptor genes. Expression of genes associated with the T cell lineage serve as indicators of commitment. We hypothesize that the human CTP expresses genes associated with human T cell development – *Gata-3*, *PTCRA*, *Rag-1*, *Rag-2*, *TCF-1*, *IL7Rα*, and *PU.1* – while being devoid of gene expression that would suggest potential in the development of other hematopoietic lineages.

Rossi et al. investigated an ABM $CD34^{+}CD7^{+}CD10^{-}Lin^{-}$ population for the expression of B cell and lymphoid-associated genes. Their study revealed that when compared to the $CD34^{+}CD7^{-}CD10^{+}Lin^{-}$ subset, $CD34^{+}CD7^{+}CD10^{-}Lin^{-}$ down-regulated the B cell specific genes *EBF* and *Pax5* while maintaining expression of the lymphoid specific genes *Rag-1*, *Rag-2*, and *CD122* (*IL-2Rβ*) (34). It should be noted that in this study, the expression of T cell specific genes was not included in their experiments. Regardless, this paper reveals that the $CD7^{+}CD10^{-}$ fraction of the human bone marrow exhibits a gene expression profile that is less B cell skewed.

In vitro experiments also lend insight into the gene expression profile of committed T cell progenitors. Awong and colleagues examined the expression of *Gata-3*, *Deltex-1*, *Rag-1*, and *Notch-1*, and *Cebpa* on $CD34^{+}CD7^{+}$ subsets generated from hHSCs 50 days after co-culture on OP9-DL1 stromal cells (7). For the purpose of our study, we

noted the expression of *Gata-3* and *Rag-1*. $CD34^+CD7^+CD1a^-$ subset expressed comparable levels of *Gata-3*, a transcription factor that is considered paramount to T lineage commitment (36, 45), to UCB $CD3^+$ T cells. This population also expressed low levels of *Rag-1* comparable to the expression level of UCB $CD3^+$ T cells. Though this phenotype was generated *in vitro* under the influence of Notch-1 ligand, the upregulation of *Gata-3* and *Rag-1* by further differentiation of $CD34^+CD7^+$ progenitors provides evidence of T cell-like gene expression activity (7).

Aside from ABM, Haddad et al. examined a $CD34^+CD45RA^{hi}CD7^+$ population in UCB for expression of T- and lymphoid linked genes (22). In an RT-PCR experiment, they demonstrate that this population expresses low levels of *Gata-3*, *Rag-1*, *PTCRA*, and *LEF-1* compared to postnatal thymocytes. However, these results were not quantified. In addition to the lymphoid associated genes, they also show that UCB $CD34^+CD45RA^{hi}CD7^+$ cells express the myeloid affiliated gene *MPO*, indicating that this population retains myeloid differentiation capacity.

Aside from gene expression, several studies have looked at the arrangement of TCRα, -β, and -δ gene segments. Evidence exists demonstrating that UCB $CD34^+CD7^+$ subsets possess rearranged TCR-δ gene segments and partially rearranged TCR-β (D-J), both of which were detected at the genomic and transcriptional level (54). These rearrangements were absent in the $CD34^+CD7^-$ fraction of the UCB, emphasizing that $CD7^+$ subsets contain T cell progenitor activity. Furthermore, this study also detected the presence of terminal deoxynucleotidyl transferase (*TdT*) in an RT-PCR experiment, verifying the gene rearrangement process in the $CD34^+CD7^+$ subset.

1.5 Objective

The objective of this work is to determine whether a committed T cell progenitor exists in the human adult bone marrow. Based on previous work done in mice (23, 43, 41), an equivalent human committed T cell progenitor population would have several distinct characteristics: They would be phenotypically more mature than $CD34^{+}CD38^{-/lo}$ hHSCs, but would be devoid of mature lineage markers. They would possess a gene expression profile that consists of T cell-associated and lymphoid-associated genes such as *Gata-3*, *TCF-1*, *PTCRA*, *IL-7Rα*, *Rag-1*, and *Rag-2*. Based on the studies discussed in this introduction, we hypothesize that the $CD34^{+}CD38^{-/lo}CD7^{+}CD10^{-}Lin^{-}$ population within the ABM is the human CTP, and present an in depth phenotypic analysis, as well as molecular evidence, that will help support, or refute, this idea.

2.1.1 Human bone marrow samples

Human mononuclear cells obtained from fresh, normal adult bone marrow were purchased from AllCells, LLC. (Emeryville, CA). Donors were between the ages of 18 and 55 years, >110 lbs, in good health, and screened for HIV, Hepatitis B and Hepatitis C before donation.

2.1.2 Antibodies and microbeads

Monoclonal mouse anti-human V450 CD7 (clone M-T701), PerCP-Cy5.5 CD34 (clone 8G12), PE-Cy7 CD38 (clone HB7), and a Human Lineage Cell Depletion Set containing biotinylated anti-human CD3 (clone UCHT1), CD14 (clone M5E2), CD16 (clone 3G8), CD19 (clone HIB19), CD41a (clone HIP8), CD56 (clone B159), and Glycophorin A (clone GA-R2) were purchased from Becton Dickinson Biosciences (San Jose, CA). Monoclonal mouse anti-human V450 CD56 (clone B159), FITC CD1a (clone HI149), FITC CD5 (UCHT2), FITC CD16 (clone 3G8), PE CD90 (clone 5E10), PE CD4 (clone SK3), PE-Cy7 CD3ε (clone UCHT1), APC CD41a (clone HIP8), APC TCRαβ (clone IP26), APC-Cy7 CD10 (clone H10a), APC-Cy7 CD14 (clone M5E2), and APC-Cy7 CD8 (clone SK1) were purchased from BioLegend (San Diego, CA). Monoclonal mouse anti-human eFluor605NC CD45RA (clone HI100), PE Glycophorin A (clone HIR2), PerCP-Cy5.5 CD45 (clone 2D1), and APC CD127 (clone eBioRDR5) were purchased from eBioscience (San Diego, CA). Monoclonal mouse anti-human FITC TCRγδ (clone IMMU510) was purchased from Beckman Coulter (Brea, CA). Monoclonal mouse anti-human FITC CCR7 (clone 150503), PE CXCR6 (clone 56811), and APC CCR9 (clone 248621) were purchased from Research & Diagnostics Systems

(Minneapolis, MN). Purified, lyophilized Mouse IgG was purchased from Sigma-Aldrich (St. Louis, MO). Streptavidin conjugated microbeads were purchased from Miltenyi Biotec (Auburn, CA). Streptavidin-PE-Texas Red microbeads were purchased from Becton Dickinson Biosciences. Anti-mouse Ig, κ/Negative control (BSA) Compensation Plus (7.5 μm) Particles Set was purchased from Becton Dickinson Biosciences.

2.1.3 Cell sorting

AutoMACS Separator was purchased from Miltenyi Biotec for cell lineage depletion. Sorts from lineage-depleted samples were performed on a BD FACSAria II Cell Sorter (Becton Dickinson Biosciences), which is equipped with 407 nm, 488 nm, and 633 nm lasers. The following filters were placed during the sorts: 450/40 and 605/40 filters for the 407 nm laser; 530/30, 575/26, 610/20, 695/40, and 780/60 for the 488 nm laser; 660/20 and 780/60 for the 633 nm laser.

2.1.3 Real-time PCR

Oligonucleotides were designed using Primer-BLAST (National Center for Biotechnology Information, Bethesda, MD) or taken from the PrimerBank (Center for Computational and Integrative Biology, Harvard University, Harvard, MA) database (sequences specified in Table 1). All oligonucleotides were purchased from Sigma-Aldrich. Binding capacity to target genes was inspected using Amplify 3 software, to ensure the absence of non-specific products or primer dimers. Oligonucleotides for real-time quantitative PCR are listed in Table 1. Reactions were performed on StepOne Plus Real-Time PCR System using Fast SYBR Green Master Mix (Applied Biosystems, Carlsbad, CA).

Table 3 – Oligonucleotides for human gene expression analysis via qPCR

Primer name	Sequence of primer (5' → 3')	Amplicon size (bp)	Accession #
h*Gata-3* forward	GTGCTTTTTAACATCGACGGTC	205	NM_002051
h*Gata-3* reverse	AGGGGCTGAGATTCCAGGG		
h*Ebf* forward	CAGCCGCTGTTGTGACAAGA	288	NM_024007
h*Ebf* reverse	AGATAAGAGGGCGTACCTTCC		
h*Rag-1* forward	TGGTCCTGTGGATGGTAAAACC	125	NM_000448
h*Rag-1* reverse	GGTGGATCGAGTCAACATCTG		
h*TdT* forward	GATGTCTCCTGGCTGATCGAA	121	NM_004088
h*TdT* reverse	CCTGGGTTGGTGCTATCTGAAT		
h*PU.1* forward	TGCCTCCAGTACCCATCCC	226	NM_003120
h*PU.1* reverse	CCACCCACCAGATGCTGTC		
h*CD3e* forward	AGGGCAAGAGTGTGTGAGAAC	112	NM_000733
h*CD3e* reverse	TCCAGTAGTAAACCAGCAGCA		
h*Id2* forward	GACCCGATGAGCCTGCTATAC	165	NM_002166
h*Id2* reverse	AATAGTGGGATGCGAGTCCAG		
h*IL7Ra* forward	CCCTCGTGGAGGTAAAGTGC	199	NM_002185
h*IL7Ra* reverse	CCTTCCCGATAGACGACACTC		
h*CD7* forward	TGGGAGCCTCCGTCAACAT	107	NM_006137
h*CD7* reverse	CCCGTCCTCGTAGTAAATGATG		
h*Tcf-1* forward	GAGGAGCAGGACGACAAGAG	292	NM_003202.3
h*Tcf-1* reverse	GCAGATTGAAGGCGGAGTAG		
h*PTCRA* forward	CACACCCTTTCCTTCTCTGG	61	NM_138296.2
h*PTCRA* reverse	CATCTGCTGCTTTCCATCC		
h*GAPDH* forward	ATGGGGAAGGTGAAGGTCG	108	NM_002046
h*GAPDH* reverse	GGGGTCATTGATGGCAACAATA		

2.1.4 PCR product cloning

pGEM-T and pGEM-T Easy Vector Systems were purchased from Promega (Madison, WI). XL1-Blue Competent cells (Agilent Technologies, Santa Clara, CA) were used for the establishment of cDNA libraries.

2.2.1 Isolation of putative human committed T cell progenitors from adult human bone marrow mobilized mononuclear cells

Mononuclear cells mobilized from human fresh, normal bone marrow from donors ages 22, 24, 26, 32, and 44, were counted by aliquoting 10 µl into a 1.5 ml Eppendorf test tube, diluting 1:20 with 0.04% trypan blue, and loading 10 µl into a hemocytometer to count. The samples were then centrifuged to remove dead cells and debris. Pelleted cells were resuspended in FACS analysis buffer (1x PBS, 5% FBS, and 0.1% sodium azide) at a concentration of 10^7 cells/50 µl buffer. In order to block the Fc (fragment, crystallizable) region on Fc receptors of cells and prevent non-specific binding of anti-human antibodies, we administered mouse IgG to a final concentration of 200 µg/ml and incubated for 10 minutes on ice. Blocked samples were stained with the biotin-labeled Human Lineage Depletion Cocktail Set (1 µl/10^7 cells) for 15 minutes on ice. After washing the cell with FACS analysis buffer, samples were centrifuged for 5 minutes at 1500 rpm and 4ºC. Pelleted cells were resuspended with 20 µl of Streptavidin microbeads per 10^7 cells and incubated in a 4ºC fridge for 30 minutes. After washing the cells with a final volume of 15 ml of FACS analysis buffer, samples were centrifuged for 10 minutes at 1500 rpm and 4ºC. Pelleted cells were resuspended in 500 µl – 1 ml of MACS running buffer (phosphate buffered saline (PBS), bovine serum albumin (BSA),

EDTA, 0.09% azide), and processed in the AutoMACS using the "DepleteS" program to separate the positive streptavidin-labeled and negative unlabeled fractions. Ten µl aliquots were taken from the lineage negative (Lin^-) fraction and diluted 1:20 with 0.04% trypan blue to determine the number of Lin^- cells. This fraction was centrifuged for 5 minutes at 1500 rpm at 4ºC. The supernatant was discarded, and pellets were resuspended at a concentration of 80 µl of FACS analysis buffer per 10^7 cells. Samples were then stained using the combination of fluorochrome-conjugated antibodies listed in Table 2.1. Individual stains are listed in Table 2.2. Concentrations for each fluorochrome-conjugated antibody were determined according to titrations done with each antibody. Mononuclear cell samples were stained with antibody cocktails for 15 minutes on ice. Samples were then washed with a final volume of 15 ml of FACS analysis buffer before centrifuging for 5 minutes at 1500 rpm and 4ºC to pellet cells. Supernatant was discarded, and pellets were resuspended at a concentration of 80 µl of FACS analysis buffer per 10^7 cells. PE-Texas Red Streptavidin microbeads were added to cell suspensions to a final concentration of 1:1600 and incubated for 15 minutes in a 4ºC fridge. Samples were washed with a final volume of 15 ml FACS analysis buffer before being pelleted at 1500 rpm, 4ºC for 5 minutes. Cells were resuspended in FACS analysis buffer at a concentration of $5x10^6$ cells/ml for sorting. Following the gating scheme shown in Figure 1, populations of interest were sorted using the 4-way sort on the FACSAria II. Sorted cells were pelleted and resuspended in Tryzol reagent (company) at a concentration of 1 ml/10^7 cells, and stored in -80ºC freezer for molecular analysis.

2.2.2 Flow cytometric data analysis using FlowJo

Cytometric data included acquiring 3 x 10^6 events from individual sorts. Flow cytometric data from each sort was analyzed using FlowJo software. Compensation on the software was done using the microbeads sample for each fluorochrome used. The percentage of putative hCTP from each bone marrow sample was recorded based on the established gating scheme (Figure 1).

Table 4.1 – Mouse anti-human antibodies and corresponding fluorochromes.

V450	eFluor 605NC	FITC	PE	PE-TxR/ PI	Per-CP Cy5.5	PE-Cy7	APC	APC-Cy7
CD7	CD45RA	CD1a CCR7 CD5	CD90 CXCR6	Lineage Dead	CD34	CD38	CD127 CD24 CCR9	CD10

Table 4.2 – Individual staining cocktails used for hCTP sorts.

V450	eFluor 605NC	FITC	PE	PE-TxR/ PI	Per-CP Cy5.5	PE-Cy7	APC	APC-Cy7
CD7	CD45RA	CCR7	CXCR6	Lineage Dead	CD34	CD38	CCR9	CD10

V450	eFluor 605NC	FITC	PE	PE-TxR/ PI	Per-CP Cy5.5	PE-Cy7	APC	APC-Cy7
CD7	CD45RA	CCR7	CXCR6	Lineage Dead	CD34	CD38	CD127	CD10

V450	eFluor 605NC	FITC	PE	PE-TxR/ PI	Per-CP Cy5.5	PE-Cy7	APC	APC-Cy7
CD7	CD45RA	CCR7	CXCR6	Lineage Dead	CD34	CD38	CD24	CD10

V450	eFluor 605NC	FITC	PE	PE-TxR/ PI	Per-CP Cy5.5	PE-Cy7	APC	APC-Cy7
CD7	CD45RA	CD1a	CD90	Lineage Dead	CD34	CD38	CD127	CD10

V450	eFluor 605NC	FITC	PE	PE-TxR/ PI	Per-CP Cy5.5	PE-Cy7	APC	APC-Cy7
CD7	CD45RA	CD1a	CD90	Lineage Dead	CD34	CD38	CD24	CD10

V450	eFluor 605NC	FITC	PE	PE-TxR/ PI	Per-CP Cy5.5	PE-Cy7	APC	APC-Cy7
CD7	CD45RA	CD5	CD90	Lineage Dead	CD34	CD38	CD24	CD10

V450	eFluor 605NC	FITC	PE	PE-TxR/ PI	Per-CP Cy5.5	PE-Cy7	APC	APC-Cy7
CD7	CD45RA	CD5	CD90	Lineage Dead	CD34	CD38	CD127	CD10

2.2.3 Establishment of cDNA library

Ligation reactions using the pGEM-T Easy Vector were performed according to the manufacturer's specifications. Reactions with PCR products at a molar-to-vector ratio of 1:1 and 3:1 were used, and incubated overnight at 4ºC to achieve a maximum number of transformants. Fifty ng of ligated plasmids were transformed into XL1-Blue competent cells following the protocol provided by Agilent Technologies.

2.2.4 Relative quantification of gene expression using qPCR

The Comparative C_T quantitation method was used with the FastSYBR Green master mix using cDNA template from sorted hHSC and hCTP populations. For T cell and lymphoid associated genes, human whole thymus was used as the positive control. For B cell, myeloid, and NK cell associated genes, whole mononuclear cells cDNA was used as a positive control. For all experiments, HeLa cDNA was used as the negative control. Reactions were run in a final volume of 20 µl per well on 96-well plates. A final concentration of 10ng of cDNA reaction from human CTP, human HSC, human thymic cDNA, and HeLa were used per 20µl reaction. A final concentration of 150 nM of each target primers was used per reaction. Each target gene and template was performed in triplicates. An initial 95 ºC step was done for 20 seconds to activate the AmpliTaq Fast DNA Polymerase. Alternating 3-second 95ºC denaturing, and 30-second 57ºC annealing and extension times for 60 cycles was used for the reactions in the StepOne Plus Real-Time PCR System. For the melting curve analysis, alternating cycles of 15-second 95ºC, 1:00 of 55ºC, followed by another 15-second 95ºC was performed once. Data from the experiments were analyzed using the software. RQ values were then plotted on Microsoft Excel to generate Figures 3 and 4.

Chapter 3 – Results

3.1 The putative human committed T cell progenitor is a rare population within the adult BM

Like the murine CTP (23, 43, 41), we speculated that human T cell progenitors in the bone marrow should be devoid of lineage surface antigens: CD3, CD14, CD16, CD19, CD41a, CD56, and CD235a. We therefore depleted Lin^+ cells from our analysis and sorts using AutoMACS as described in the Materials and Methods chapter. Based on our cell counts prior and post-MACS depletion, the fractionated Lin^- subpopulation, on average, comprised 13±3% of our bone marrow samples.

A number of studies utilized CD34 as a marker for immature T cell progenitors from fetal and adult tissues (64, 61, 22, 60, 30, 62). We therefore gated and analyzed the $CD34^+$ fraction of the Lin^- bone marrow population (Figure 1). Several studies have shown that the total $CD34^+$ population within the bone marrow is 1-5% (58, 63). However, these percentages describing the frequency of $CD34^+$ cell reported in these studies do not account for the depletion of the Lin^+ population. The mean percentage of $CD34^+Lin^-$ observed from our five experiments was 0.65±0.55% of the total bone marrow cells.

Studies have claimed that differences in CD38 expression can be used to isolate T cell progenitors within $CD34^+$ cells (7, 47). However, these studies present contradictory evidence for the presence and abundance of CD38 on T cell progenitors in the bone marrow. We therefore sought to investigate the $CD34^+Lin^-$ subsets based on the expression of CD38 (Figure 1). On average, the $CD38^{-/lo}$ fraction of the $CD34^+Lin^-$ subset comprised 0.27±0.24% of the total bone marrow sample, while the $CD38^{hi}$ fraction made

up less than 0.005%. We observed that the $CD38^{-/lo}$ fraction was heterogeneous in terms of their side scatter (SSC) profile, comprised of distinct SSC^{high} and SSC^{med} populations (Figure 1). We analyzed these different subsets separately; however, their cell numbers are markedly reduced, rendering any results difficult to interpret.

We examined the expression of CD7 and CD10 within each CD38 population. We found that the majority of the $CD7^{+}CD10^{-}$ subset is contained in the $CD38^{-/lo}$ fraction, while the human $CD34^{+}CD38^{hi}CD7^{-}CD10^{+}Lin^{-}$ common lymphoid progenitor (CLP) (55) is found within the $CD38^{hi}$ fraction (Figure 1). Furthermore, the $CD38^{-/lo}$ fraction contained few, if any, $CD10^{+/hi}$ cells, but contained a majority of the $CD7^{+}$ populations. We observed that the $CD34^{+}CD38^{-/lo}CD7^{+}CD10^{-}Lin^{-}$ hCTP, on average, comprises 0.04±0.03% of the total human bone marrow (Table 3). However, the range varied from 0.01% to 0.1%, depending on the donor's age. This percentage makes the putative hCTP a much rarer population when compared to the $CD34^{+}CD38^{-/lo}Lin^{-}$ hHSCs, which was found at an average 0.27±0.23% of the total bone marrow.

Figure 1 – The putative human CTP is found exclusively within the $CD34^{+}CD38^{-/lo}$ subpopulation. Representative FACS plots showing the gating scheme for sorted Lineage-depleted bone marrow mononuclear cells. Human CTP ($CD34^{+}CD38^{-/lo}CD7^{+}CD10^{-}$ ■), hHSC ($CD34^{+}CD38^{-/lo}$ ■), and hCLP ($CD34^{+}CD38^{+/hi}CD7^{+}CD10^{-}$ ■) shown with shaded gates. $n = 5$.

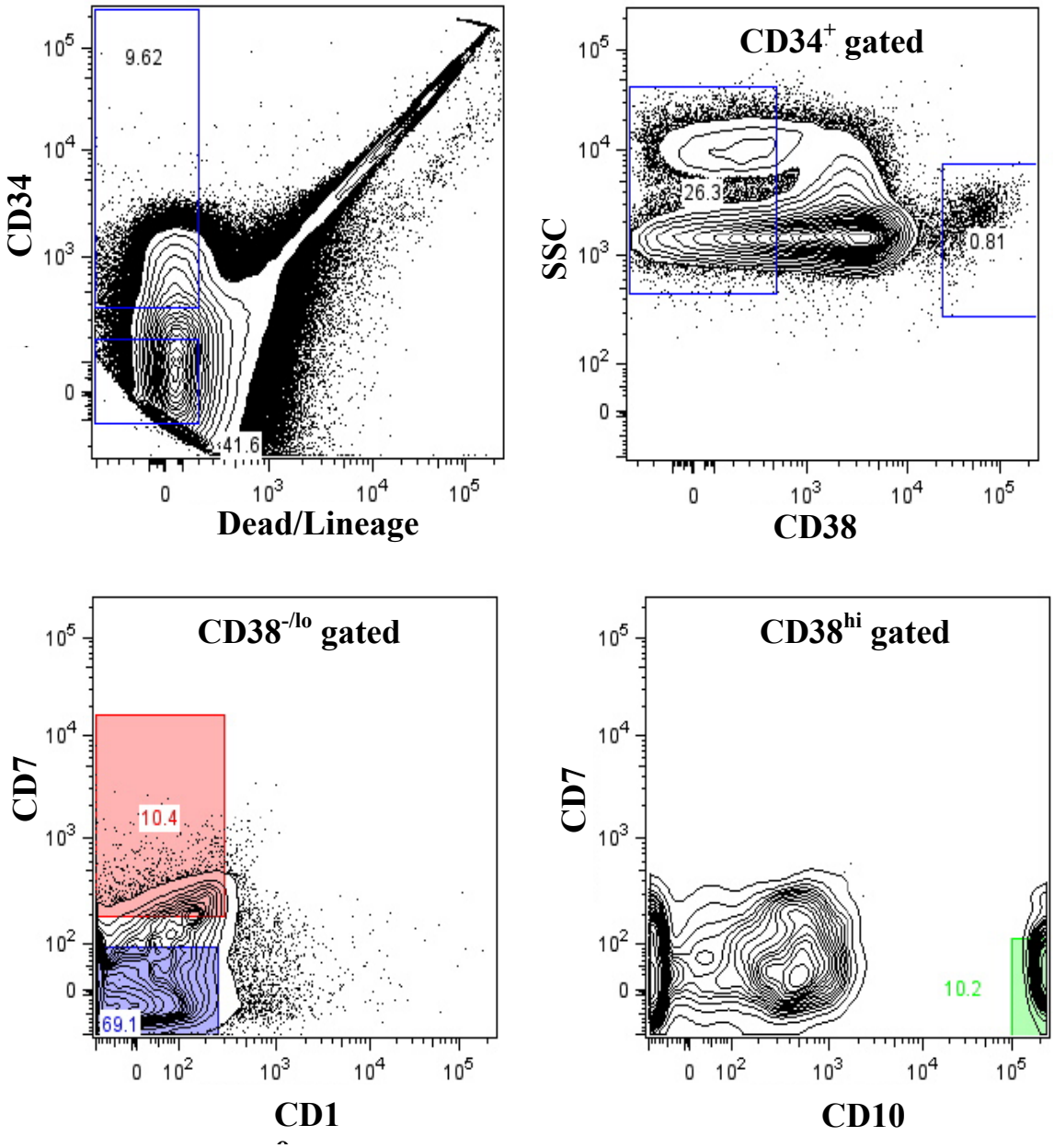

Table 3 – The putative hCTP is a rare population within ABM (n = 5).

Experiment #	**Donor Age**	**$CD34^{+}CD38^{-/lo}CD7^{+}Lin^{-}$**
1	22	0.026
2	32	0.013
3	21	0.095
4	32	0.065
5	38	0.020
Average	**29**	**0.044**
Standard Deviation	**9**	**0.035**

3.2 Phenotypic analysis of the putative human committed T cell progenitor

We have identified a rare $CD34^{+}CD38^{-/lo}CD7^{+}CD10^{-}Lin^{-}$ population within the adult human bone marrow. Using multi-color flow cytometry, we extensively investigated this $CD34^{+}CD38^{-/lo}CD7^{+}CD10^{-}Lin^{-}$ population for the presence of T cell and lymphoid associated surface markers, as well as chemokine receptors. For staining protocols and cocktails, refer to Materials and Methods. Representative plots for each surface marker are shown in Figure 2.

CD5 and CD1a serve as surface markers associated with thymic T cell development (49, 59, 62, 64). Figure 2A (left panel) shows that CD5 is expressed at nearly equal intensities on our putative $CD34^{+}CD38^{-/lo}CD7^{+}CD10^{-}Lin^{-}$ hCTP and the $CD34^{+}CD38^{-/lo}CD7^{-}CD10^{+}Lin^{-}$ hCLP. The level of expression observed for CD5 in both populations were relatively equal between the two populations as well; however, both the putative hCTP and hCLP display a distinct increases in CD5 expression when compared to the $CD34^{+}CD38^{-/lo}$ hHSC population and unstained background control. We observed a similar pattern with CD1a expression. The intensity peaks for CD1a expression in both the hCTP and hCLP are only slightly shifted from the hHSC and unstained control samples, and are nearly identical (Figure 2A, right panel).

We investigated the hCTP and hCLP populations for the abundance of several lymphoid-associated surface markers. CD127 (IL-7Rα) has been implicated as essential for normal T cell development, as IL-7Rα-deficient patients lack T cells (48). In addition, early thymic $CD34^{+}$ T/NK precursors have been shown to express surface CD127 (39). In our experiments, we observed that the hCTP expressed low levels of CD127 on their cell

surface, when compared to the hHSC and unstained samples. This contrasts to the hCLP, which we found to be consistently $CD127^{hi}$ (Figure 2B, left panel). Several groups utilized CD45RA to fractionate human bone marrow in search of T cell precursors (57, 22). Our $CD34^{+}CD38^{-/lo}CD7^{+}CD10^{-}Lin^{-}$ putative hCTP and $CD34^{+}CD38^{-/lo}CD7^{-}CD10^{+}Lin^{-}$ hCLP populations expressed cell surface CD45RA (Figure 2B, middle panel). The shifts in the peaks of these two populations are nearly overlapped by the broad peak of the hHSC. However, when compared to the unstained sample, these three peaks show a distinct shift.

Previous studies have shown that CD24 expression occurs in early B cell progenitors, even before expression of cell surface CD19 (24). We therefore included CD24 in our phenotypic analysis and discovered differential surface expression of this marker between the hCTP and hCLP populations (Figure 2B, right panel). Specifically, the abundance of CD24 surface expression was nearly 1000-fold higher in the hCLP than hCTP.

In addition to T cell and lymphoid-associated surface markers, we probed for the expression of chemokine receptors involved with T cell progenitor migration to the thymus. The chemokine receptors CCR7 and CCR9 have been well documented to be involved with colonization of the murine thymus (27, 29). The hCTP population exhibited the greatest shift in fluorescent intensity of CCR7 over the unstained background, though the hCLP population did possess a lesser degree of the chemokine receptor (Figure 2C, left panel). We also examined the sorted populations for cell surface expression of CCR9, and find that this chemokine receptor is exclusively expressed at the cell surface of the putative hCTP population (Figure 2C, right panel). We also examined

surface expression of CXCR6 on both the hCTP and hCLP populations. We reasoned that since CXCR6 is expressed solely on murine CTPs (Drs. Jennifer Manilay and Marcos E. García-Ojeda, personal communication), human CTPs may also express this chemokine receptor. Our experiments mirror the murine data, showing that CXCR6 is exclusively expressed on the hCTP while being absent on the hCLP and hHSC populations (Figure 2C, middle panel).

Figure 2 – The putative hCTP expresses T cell and lymphoid associated surface markers, and chemokines associated with thymic migration. Cell surface analysis of hCTP ( ), hHSC ( ), and hCLP ( ). Shown are representative plots for expression of **(A.)** T cell associated markers CD5 and CD1a, **(B.)** lymphoid lineage associated markers CD127, CD45RA, and CD24, and **(C.)** Chemokine receptors CXCR6, CCR7, and CCR9 – associated with migration from human bone marrow to the thymus ($n = 5$).

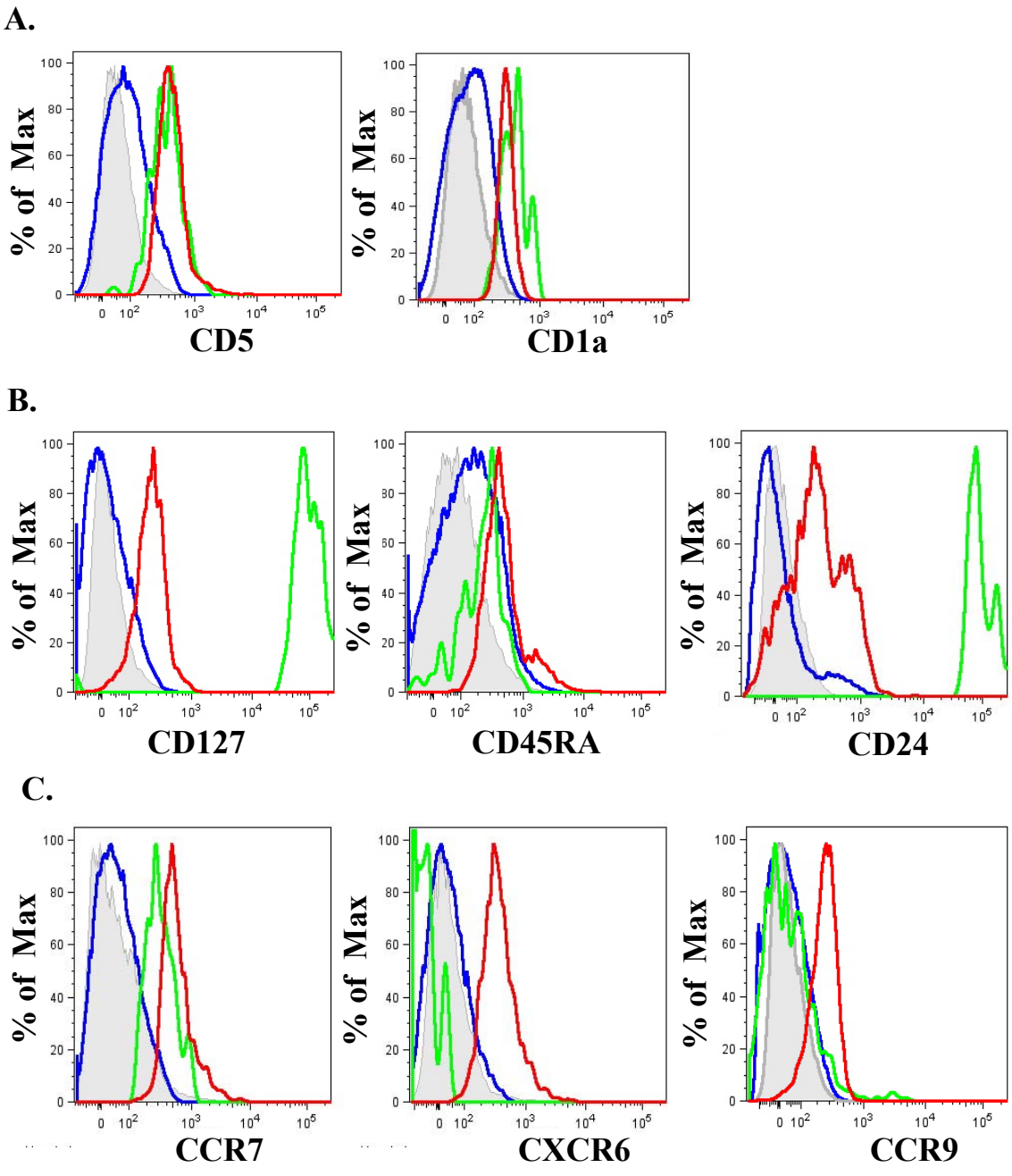

3.3 Molecular analysis of the putative human committed T cell progenitor

The phenotypic analysis of cell surface makers provides only one facet of our characterization of our $CD34^{+}CD38^{-/lo}CD7^{+}CD10^{-}Lin^{-}$ putative hCTP population. In addition to phenotypic analysis, we also analyzed the gene expression profile of our putative hCTP.

The transcription factor GATA-binding protein 3 (*Gata-3*) is widely recognized as an essential transcription factor for T cell progenitor survival and expansion within the thymus (36, 45). We wanted to determine whether the putative hCTP expressed *Gata-3*. Figure 3A shows that the hCTP is devoid of *Gata-3* expression. Human HSCs displayed relatively high amount of *Gata-3* compared to the human whole thymus cDNA. As expected, the relative quantity of *Gata-3* in our HeLa samples was lowest. This observation is recapitulated in the melting curve analysis plot for *Gata-3* (Figure 6A), in which low levels of *Gata-3* transcripts are observed in human thymic, hHSC, and HeLa cDNA. In addition, the primer set for this gene appeared specific, given the fact that no other peaks were generated other than the background in the melting curve analysis (Figure 6A).

In vitro experiments have shown that CD7 is quickly upregulated when $CD34^{+}CD38^{-/lo}$ hHSCs are co-cultured on OP9-DL1 stroma (2, 7). We therefore reasoned that the hCTP, in addition to displaying CD7 on the cell surface, would have CD7 transcripts present intracellularly. However, this reasoning proven incorrect, as CD7 is absent from our sorted hCTP populations (Figure 3B). As expected, the human whole thymus positive control expresses CD7, while expression is lowest in the HeLa control

(Figure 3B). Additionally, the hHSC population exhibited little to no expression in relative to the thymic and HeLa control samples (Figure 3B). We also show here that the qPCR reactions for CD7 generated only a single peak for the populations examined; indicating that the primer set amplified its specific target product (Figure 6B). Unexpectedly, the melting curve analysis reveals that at least one of the three triplicates in each sample generated a peak for CD7 (Figure 6B), including the HeLa negative control, which generated a peak comparable to the thymic cDNA samples.

The presence of CD3ε is another hallmark of T cell commitment. Galy and colleagues have shown that the earliest $CD34^{+}CD1a^{-}$ thymocytes express cytoplasmic CD3ε (62). Klein et al. identified a $CD34^{+}CD38^{-}Lin^{-}CD7^{+}CD10^{+}$ population that expresses preTα and pre-TCR complexes on their cell surface, leaving open the presence CD3ε transcripts (33). We, therefore, wanted to determine whether our putative hCTP expresses intracellular CD3ε. As shown in Figure 3C, CD3ε is absent in both the hHSC and putative hCTP populations. Not surprisingly, the human thymic positive control displayed on average a 15-fold increase over the negative control HeLa sample. However, it is interesting when considering the melting curve analysis for CD3ε. One of the three hCTP triplicates generated the appropriate curve for CD3ε (Figure 6C), but this is not reflected in the gene analysis plot. One of the triplicates of the hHSC sample generated a non-specific curve, which may be a result of poor primer design.

Previous studies have shown that a subset of $CD34^{+}CD7^{+}$ cells within the human umbilical cord blood exhibit T cell receptor gene rearrangement (54). To test for evidence of TCR gene rearrangement, we included in our molecular analysis *Rag-1*, which is involved with gene rearrangement processes in lymphoid lineage cells. As shown in

Figure 3D, the putative hCTP lacks expression of *Rag-1* when compared to the whole thymus positive control. This observation is further backed by the melting curve analysis shown in Figure 6D. Peaks appear for human thymic cDNA samples, but not for hCTP samples. Surprisingly, one of the triplicates for the hHSC sample generated a similar peak as those seen in the thymic sample, and HeLa sample generated non-specific peaks (Figure 6D). However, these peaks are not reflected in Figure 3D, in which *Rag-1* is exclusively detected in thymic cDNA samples.

A committed T cell progenitor expresses T cell and lymphoid associated genes, while being devoid of genes associated with other hematopoietic lineages. Therefore, we tested the putative hCTP for expression of genes involved with differentiation of other hematopoietic lineages. One of these genes includes *PU.1*, a transcription factor required for early granulopoiesis by common myeloid progenitors (38). As shown in Figure 4A, the putative hCTP expresses the transcription factor *PU.1* relative to the whole mononuclear cells positive control and HeLa negative control. The hHSC population also displayed on average a 50-fold increase to the negative control HeLa in the amount of *PU.1* expressed. This observation is substantiated by the melting curve analysis of products produced from the reaction (Figure 7A), showing the same products of the reactions in all the samples except for the negative HeLa control.

Id2 is a helix-loop-helix DNA binding inhibitor has been shown to have roles in multiple differentiation processes (4, 3, 26), but is most recognized as an NK-associated protein. Our putative hCTP, on average, expresses nearly a 20,000-fold increase to the HeLa sample (Figure 4B). This average was more than the hHSC and MNC.

Surprisingly, the negative control HeLa sample generated a positive peak similar to the hCTP, hHSC, and MNC samples in the melting curve analysis (Figure 8B).

Figure 3 – The putative hCTP does not express T cell and lymphoid associated genes. Relative quantification of (A) *Gata-3*, (B) CD7, (C) CD3ε, and (D) *Rag-1* transcripts from cDNA of sorted populations: hCTP, hHSC, human whole thymus, and HeLa. $n = 2$. Lines indicate the mean for triplicates. Representative plots are shown.

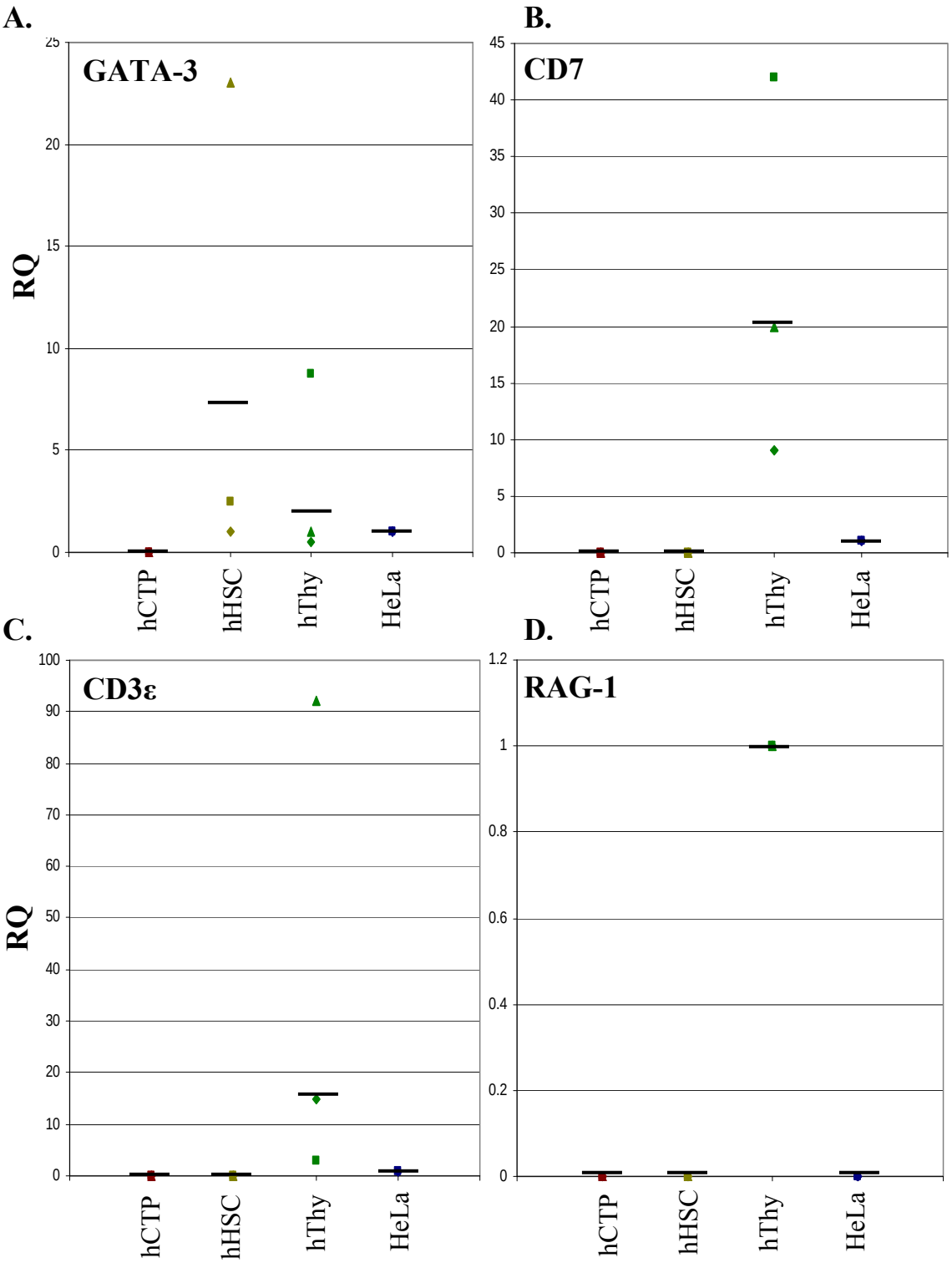

Figure 4 – The putative hCTP expresses *PU.1* and *Id2*. Relative quantification of (A.) *PU.1* and (B.) *Id2* from cDNA of sorted populations: ■ hCTP, ■ hHSC, ■ whole mononuclear cells (MNC), ■ HeLa. *n* = 2. Lines indicate the mean for triplicates. Representative plots are shown.

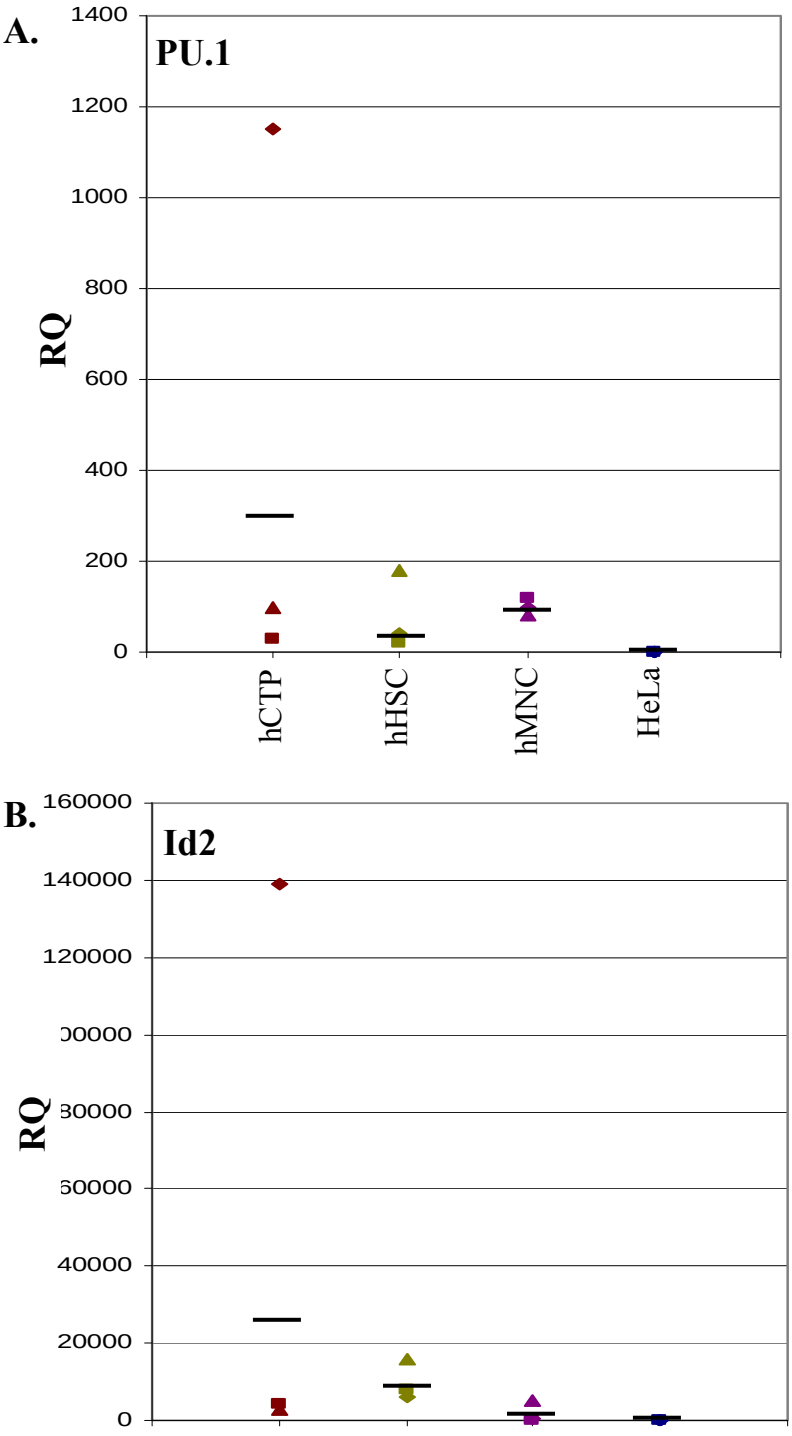

Figure 5 – Melting curve analysis of qPCR products from GAPDH reactions reveals different levels of expression between samples and individual experiments. ■ hCTP, ■ hHSC, ■ human whole thymus, ■ MNC, ■ HeLa. $n = 2$

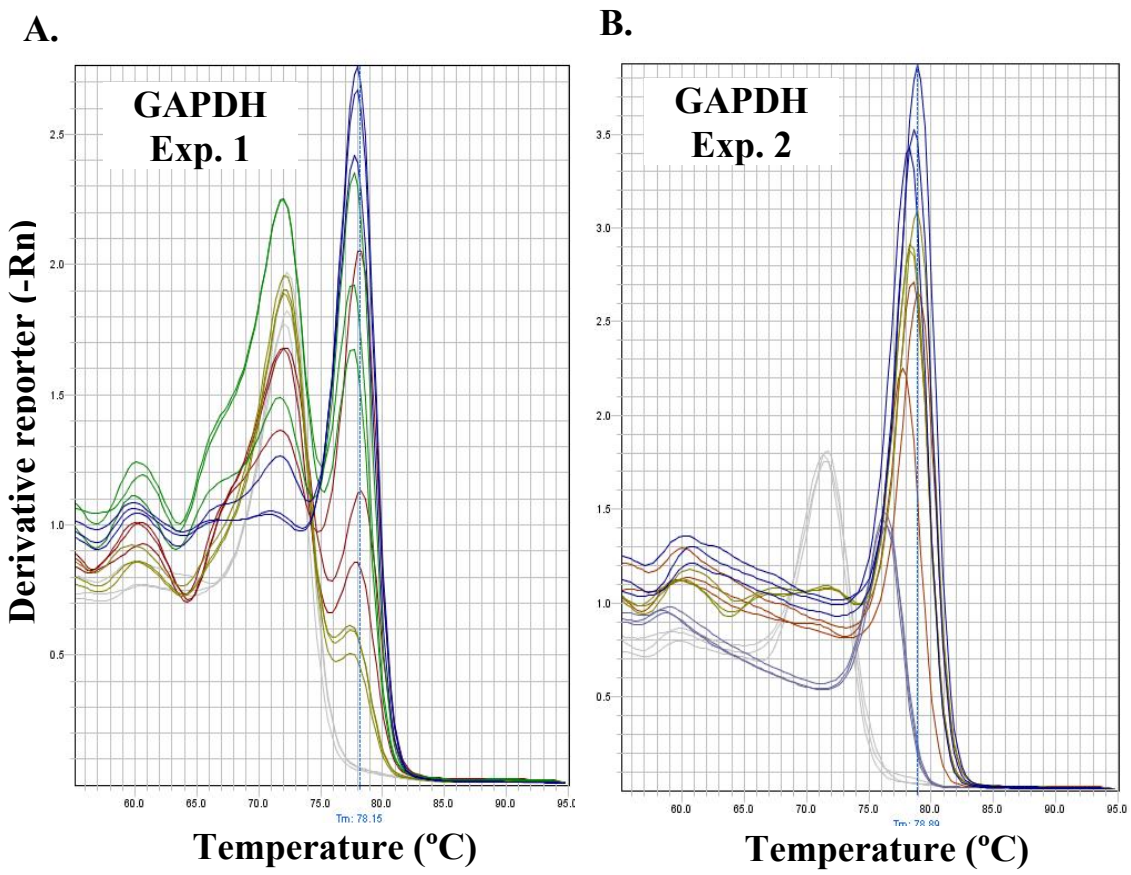

Figure 6 – Melting curve analysis of qPCR products from (A) *Gata-3*, (B.) CD7, (C.) CD3ε, and (D) *Rag-1* reactions. hCTP, hHSC, human whole thymus, HeLa. $n = 2$. Representative plots are shown.

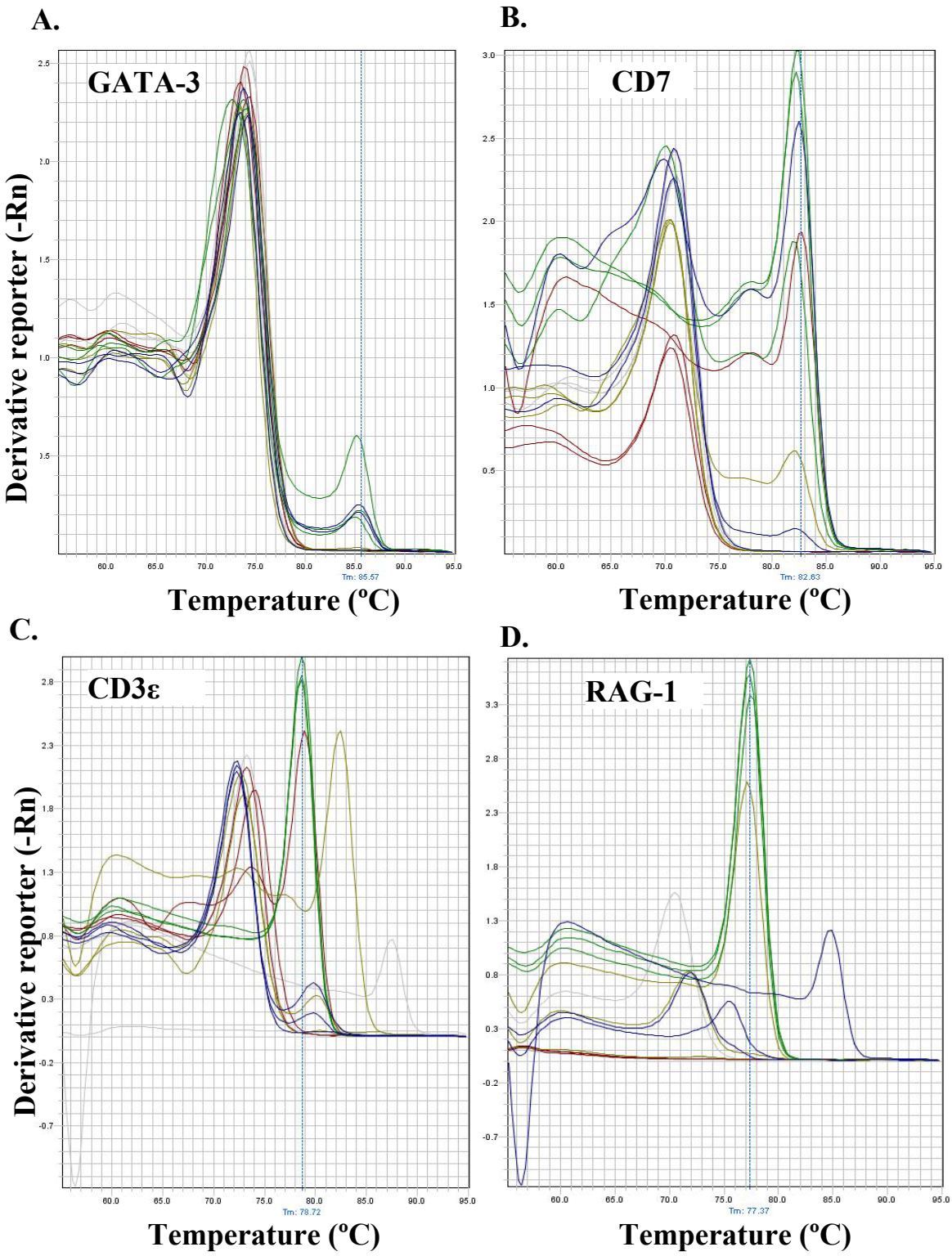

Figure 7 – Melting curve analysis of qPCR products from (A) *PU.1* and (B.) *Id2* reactions. hCTP, hHSC, MNC, HeLa. $n = 2$. Representative plots are shown.

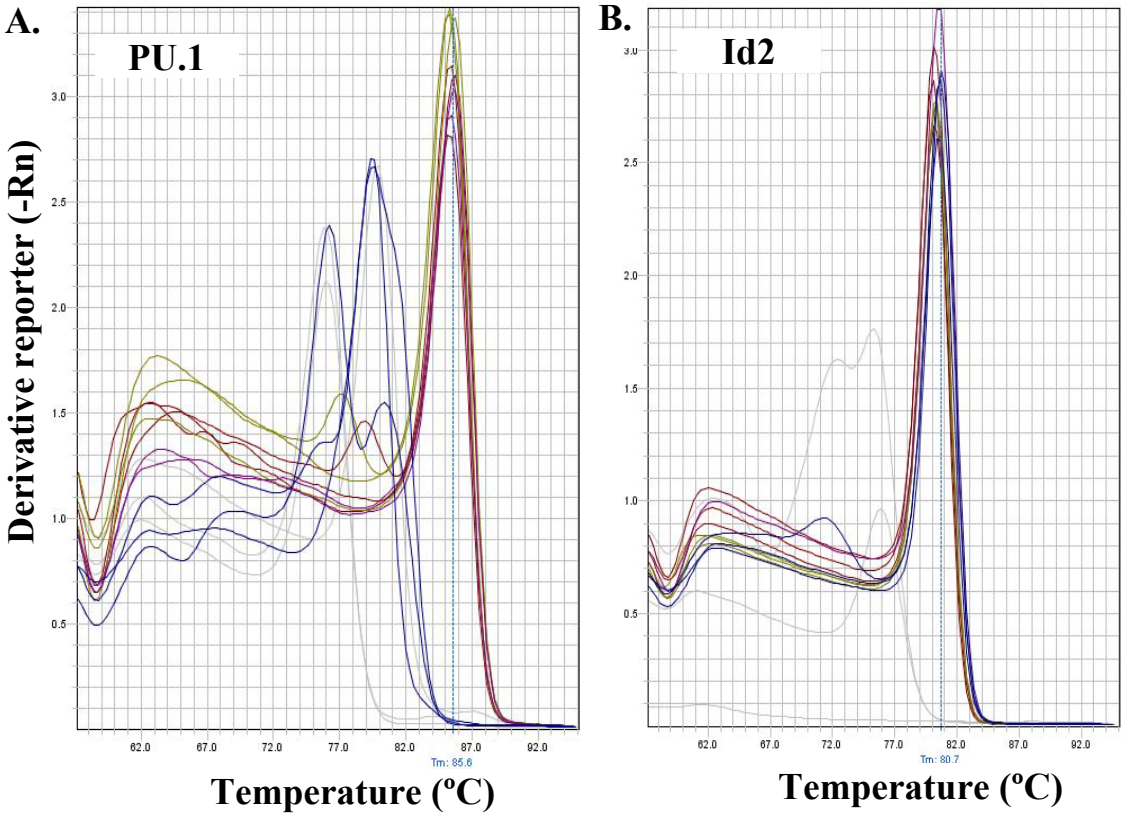

Chapter 4 – Discussion

The data presented in Chapter 3 identified a human committed T cell progenitor through phenotypic and molecular characterization. We based our gating strategy on the studies highlighted in the introduction, and identified a $CD34^{+}CD38^{-/lo}CD7^{+}CD10^{-}Lin^{-}$ population within the ABM. Our phenotype analysis reveals that our putative hCTP possesses surface markers similar to those of the characterized human early thymic progenitor (70, summarized in Table 6). Briefly, the putative hCTP and human early thymic progenitor (hETP) both possess CD34, CD45RA, the early T cell surface markers (CD7, CD2, and CD5), and IL-7Rα, while having little to no cell surface CD38. However, the major distinction between these two populations based on the surface markers investigated is the expression of CD1a on the cell surface of the hCTP. Early thymocytes upregulate CD1a intrathymically (64), and $CD34^{+}CD38^{+}CD1a^{+}$ thymocytes correlate to the DN3 stage, which have rearranged TCRδ (V-DJ), TCRγ, and TCRβ (D-J) loci (25). Further experiments, such genomic PCR, to determine the arrangement of the TCRδ, –γ, and –β loci would clarify whether our putative hCTP possesses a similar level of T cell commitment as $CD34^{+}CD38^{+}CD1a^{+}$ thymocytes.

Currently, few studies in literature have investigated chemokine receptors as a possible indicator of thymic migration. All three chemokine receptors investigated in this project were present on our putative hCTP. Among the recognized chemokine receptors important for homing to the thymus are CCR7 and CCR9 (9, 44, 31). In addition, surface expression of CXCR6 has been observed on mCTP (Drs. Jennifer Manilay and Marcos E. García-Ojeda, personal communication). Cell surface expression of these chemokine receptors suggests that this population may be capable of thymus immigration. However,

the ability for our putative hCTP to reconstitute the thymus cannot be determined by phenotypic analysis alone, and would require *in vivo* transplantation or an FTOC experiment to make any significant conclusions.

Similar to the murine CTP, the putative hCTP expresses detectable levels of CD24. Six and colleagues used CD24 expression to identify committed B cell progenitors from the ABM (15), while another study found that CD24 is expressed at the cell surface of $CD19^{-}CD79a^{+}$ early B cell progenitors (24). Therefore, the surface expression of CD24 on our putative hCTP requires further investigation on the significance of this B cell lineage associated surface marker. One avenue we could pursue is to co-culture our putative hCTP population on OP9 stroma with hFlt3L and hIL-7 to promote B cell differentiation. This would help clarify the potential of the putative hCTP to differentiate into the B cell lineage.

The IL-7R is thought to be indispensible for human T cell development, as thymocytes cannot proceed past the $CD34^{+}CD1a^{+}$ stage of development when grown in an FTOC with an anti-IL-7Rα antibody (50). The presence of CD127 on the putative hCTP may suggest that this population is also dependent on IL-7 for survival. Our proposed functional assay with co-culture conditions to promote T cell differentiation (OP9-DL1 stroma with IL-7) could be modified to lack IL-7 cytokine treatment to test this idea.

To our knowledge, molecular characterization of the hETP has not been made by previous studies. On the other hand, the gene expression profile of the murine ETP has been studied, and serves as a comparison to our putative hCTP. Table 7 summarizes the gene expression profile of the putative hCTP and the characterized murine ETP (71).

Noteworthy is the similarity between the two populations for the expression of *PU.1* and *Id2*. Traditionally associated with early granulopoiesis and monopoiesis (19), *PU.1* expression is also required by progenitor populations that migrate to the thymus, and detectable levels remain through the early intrathymic $CD34^{+}CD7^{+}Lin^{-}$ and DN stages (10, 12). *Id2* in early thymocytes promotes differentiation of thymic progenitor cells into a $CD1^{-}CD5^{+}$ NK progenitor phenotype, and eventually into mature NK cells, while inhibiting T cell development (3). One way *Id2* exerts its effects on thymocyte development is by sequestering *E2A*, which is involved in T cell lineage commitment at an early stage of thymocyte development, and has been shown to be a positive regulator of *Gata-3* (71). Isolation of early thymocytes using the same antibodies used for isolating the putative hCTP through flow cytometry would allow us to compare their gene expression profiles for expression levels of *PU.1* and *Id2*. Furthermore, we could also relatively quantify the level of *E2A* transcripts between the putative hCTP and human thymocytes to clarify the significance of *Id2* and *PU.1* expression. Finally, based on our preliminary data, the putative hCTP's lack of *Gata*-3 expression differs from the murine ETP. This would suggest a lack in T cell lineage commitment. However, as discussed shortly, this result may not be accurate based on inadequate reaction conditions and inappropriate controls.

Table 6 – Comparison of the surface marker expression between the putative hCTP and hETP.

Surface marker	**Population**	
	Human early thymic progenitor [70]	**Putative hCTP**
CD34	+	+
CD38	-	-/lo
CD7	+	+
CD1a	-	+
CD2	+	?
CD5	+	+
IL-7Rα (CD127)	+	+
CD45RA	+	+
CD44	+	?
CD33	-	?

Table 7 – Comparison of the gene expression profile between the putative hCTP and mETP.

Gene	**Population**	
	Murine early thymic progenitor [71]	**Putative hCTP**
PU.1	+	+
Id2	+	+
SCL (TAL1)	+	?
Gata-2	+	?
Gata-3	+	-
Tcf-7	+	?
Hes1	+	?
Rag-1	-/lo	-

It must be noted that we employed the comparative C_T ($\Delta\Delta C_T$) method when performing the real time PCR analysis. This method is a relative quantitation of gene expression based on a calibrator or internal control gene, and makes the assumption that the reaction efficiency for all primer pairs is 1 (13). These results give an idea of the relative gene expression profile of our populations in question and provide the basis for future experiments (see future directions), but do not give an absolute quantitation of gene expression between our sorted populations. Therefore, the first step in order to adequately evaluate our qPCR data would be to perform the standard analysis experiments to ensure that the all primer pair reaction efficiencies are equal to 1.

Our negative control HeLa samples expressed *Gata-3*, *CD7*, and *Id2*. Based on previous literature, human *Gata-3* was not detected in the HeLa cell line (65). Through hypersensitivity site assays, it has been shown that *CD7* is not expressed in HeLa cells as well (66). Our real-time PCR data contradicts these observations. In fact, companies such as Abcam and Santa Cruz Biotechnology have isolated antibodies specific for human *Gata-3* (http://www.abcam.com/GATA3-antibody-ab32858.html) and *CD7* (http://www.scbt.com/datasheet-19606-cd7-3a1e-12h7-antibody.html), and used HeLa whole cell and nuclear extract respectively as positive controls. Upon further inspection, *Id2* has been shown to be expressed on the HeLa cell line (6). It is apparent that we must use a different negative control for future real-time PCR experiments in order to generate accurate results, as the comparative C_T method normalizes all relative quantity values to the negative control.

Another concern with the qPCR data comes from our variation of expression in the GAPDH control. Clearly the level of expression of GAPDH is not equal between

samples, and also between experiments, as shown by the melting curve analysis from two experiments. All reverse transcribed RNA was quantified using a Nanodrop under a constant setting of 33 to obtain single stranded cDNA concentration, and properly diluted to a 100 ng/µl working stock solution. Error may have occurred at this step of experimentation, resulting in uneven dilution between GAPDH cDNA between samples. However, there is the possibility that GAPDH may have been a poor reference gene. Sabek et al. demonstrated that comparing the RNA of several housekeeping genes to total human (calibrator) RNA using two-step RT-PCR resulted in a ΔC_T variation in GAPDH expression on average of 4 cycles (37). Therefore, testing for the use of another housekeeping gene may be something to consider for further gene expression analysis experiments.

For the genes that produced positive peaks in our qPCR reactions, there are a couple approaches available to us to ensure that the amplicons are indeed the intended amplicons. The first would be to run the qPCR products along with a 100 base pair marker with known amplicons sizes. This would allow us to visually determine the size of the qPCR amplicons. An alternative method would be to send our amplicons for sequencing. The sequence of the amplicons can then be compared to the NCBI database using BLAST to check for sequence alignments.

One other consideration in regards to our experiments was the amount of cells, and thus transcriptional and cellular material, that we could obtain from our sorts. On average, we sorted 40,000 putative hCTPs per 2 x 10^8 whole mononuclear cells based on our gating scheme. This low number of cells yielded low amounts of RNA per sort, limiting our quantitative PCR experiments in the template maximum concentration (20

ng cDNA/test). In addition, our gating scheme for the hCLPs yielded less than 10,000 cells per 2 x 10^8 whole mononuclear cells. This made testing this population for gene expression by conventional qPCR approaches nearly impossible due to the low amount of RNA that we obtain from our sorted hCLPs. Multiplex, single cell RT-qPCR could be used to examine the gene profile of this rare population.

To definitively demonstrate that our putative hCTP is committed to the T cell lineage, we could perform a functional test of this ABM population using OP9-DL1 stroma as described previously (72). Briefly, we would co-culture OP9-DL1 stroma with our isolated putative hCTP. Human *in vitro* co-culture experiments require between $5x10^3$ – $1x10^4$ stem cells seeded per well (72). The co-culture would be grown in α-Modified Eagle's Medium (α-MEM) supplemented with 20% heat-inactivated FBS, 1x Penicillin/Streptomycin, 5 μg/ml hIL-7, and 5 μg/ml hFlt-3L. After 1, 2, 4, and 8 weeks, the cells will be harvested and analyzed by flow cytometry for the expression of immature and mature T cell markers to evaluate the developmental progress of the cultured progenitors (7). B-, NK-, and myeloid lineage potential will be evaluated by the expression of CD19, CD56 and CD14, respectively. However, low cell numbers would greatly limit the amount *in vitro* co-cultures that we could perform, so miniaturization using our putative hCTP of the co-culture experiment to produce more replicates would be necessary. This may increase the amount of time for mature T cells to develop (14). Furthermore, the question of whether the putative hCTPs could be used in a clinical setting would need to be tested.

Similarly, NK- and B cell potential would be demonstrated by co-culturing the putative hCTP with OP9 stroma supplemented similarly to the OP9-DL1 co-culture (see

above). However, to test for NK potential, we would co-culture with hIL-15 (22, 34) in addition to hIL-7. After 1, 2, 4, and 8 weeks, we would sort the populations using the same approach mentioned for the OP9-DL1 co-culture to evaluate the lineage potential under this culture condition.

In addition to lymphoid lineages, we would test for the putative hCTP population's capacity to differentiate into myeloid lineage cells. The putative hCTP will be assayed by culture on human methylcellulose enriched media (R&D Systems, Minneapolis, MN). This media contains recombinant human rhSCF (50 ng/ml), rhGM-CSF (20 ng/ml), rhG-CSF (20 ng/ml), rhIL-3 (20 ng/ml), rhIL-6 (20 ng/ml) and rhEpo (3 IU/ml) and allows for the development of CFU-E, CFU-G, CFU-GM, BFU-E, CFU-M, and CFU-GEMM. Putative hCTPs and hHSCs will be plated in triplicates and will be scored for each colony type after 14 days of culture.

Chapter 5 – Conclusions

The work presented in this thesis aims at addressing questions about the existence and identity of a human committed T cell progenitor within the adult bone marrow. Previous work in mouse has identified a murine committed T cell progenitor population within the bone marrow that is more mature than the murine hematopoietic stem cell. Molecular analysis revealed that the mCTP exhibit a gene expression profile expected of a T cell progenitor, with *PTCRA*, *Rag-1*, *Rag-2*, *Gata-3*, *TCF-1*, *IL-7Rα*, and sterile Cβ transcripts present (23, 41, 43).

In the search for a human equivalent population, we identified an ABM $CD34^{+}CD38^{-/lo}CD7^{+}CD10^{-}Lin^{-}$ population with low cell surface expression of CD5 and CD1a, an overall phenotype resembling early human thymocytes (49, 59, 62, 64). In addition, this population expresses CD127 (IL7Rα) and CD45RA, which are expressed at the cell surface of early T cell precursors (60, 48, 50, 57, 22). Further exhaustive phenotype analysis revealed that this population expresses low levels of chemokine receptors implicated in thymic migration on its cell surface: CCR7, CCR9, and CXCR6 (9, 44, 31, Drs. Jennifer Manilay and Marcos E. García-Ojeda, personal communication).

Our molecular analysis further reveals that this population expresses *PU.1* and *Id2*, similar to the murine early thymic progenitor (71) and early human thymocytes (3, 10, 12). The significance in the expression of these two transcription factors in putative hCTP requires further clarification by comparing the levels of expression in the hCTP to those found in early human thymocytes. For now, our preliminary data establishes a comparison in gene expression profile to characterized progenitor populations. Unlike the murine CTP, our preliminary data would suggest that the putative hCTP lacks expression

of T cell and lymphoid associated genes *Gata-3*, *CD7*, *CD3ε*, and *Rag-1*. However, as noted in the discussion, several adjustments to our qPCR experiments must be made before we can confidently interpret our gene expression data. This includes a standard curve experiment to ensure the quality of our primer sets and reaction conditions, redesigning the primer pairs or further optimizing the reaction conditions for the genes that did not produce our expected amplicons, confirming the products for genes that worked, and using a different negative control in place of the HeLa cell line.

Based on our phenotypic and molecular results, we conclude that this ABM $CD34^{+}CD38^{-/lo}CD7^{+}CD10^{-}Lin^{-}$ putative hCTP population resembles an early thymic progenitor. However, *in vitro* differentiation assays to test the lineage potential of the putative hCTP would establish the level of T cell commitment by the population.

Chapter 6 – Bibliography

1. Roncarolo MG, Gregori S, Lucarelli B, Ciceri F, Bacchetta R. Clinical tolerance in allogeneic hematopoietic stem cell transplantation. *Immunol Rev.* 2011 May; 241 (1) :145-63. PubMed PMID:21488896.
2. De Smedt M, Leclercq G, Vandekerckhove B, Kerre T, Taghon T, Plum J. T-lymphoid differentiation potential measured in vitro is higher in CD34+CD38-/lo hematopoietic stem cells from umbilical cord blood than from bone marrow and is an intrinsic property of the cells. *Haematologica*. 2011 May; 96 (5) :646-54. PubMed PMID:21330325; PubMed Central PMCID: PMC3084910.
3. Schotte R, Dontje W, Nagasawa M, Yasuda Y, Bakker AQ, Spits H, Blom B. Synergy between IL-15 and *Id2* promotes the expansion of human NK progenitor cells, which can be counteracted by the E protein HEB required to drive T cell development. *J Immunol.* 2010 Jun 15; 184 (12) :6670-9. PubMed PMID:20483740.
4. Ramirez K, Kee BL. Multiple hats for natural killers. *Curr Opin Immunol.* 2010 Apr; 22 (2) :193-8. PubMed PMID:20335012.
5. Mandel EM, Grosschedl R. Transcription control of early B cell differentiation. *Curr Opin Immunol.* 2010 Apr; 22 (2) :161-7. PubMed PMID:20144854.
6. Manthey C, Mern DS, Gutmann A, Zielinski AJ, Herz C, Lassmann S, Hasskarl J. Elevated endogenous expression of the dominant negative basic helix-loop-helix protein ID1 correlates with significant centrosome abnormalities in human tumor cells. *BMC Cell Biol.* 2010 Jan 14; 11:2. PubMed PMID:20070914; PubMed Central PMCID: PMC2818612.

7. Awong G, Herer E, Surh CD, Dick JE, La Motte-Mohs RN, Zúñiga-Pflücker JC. Characterization in vitro and engraftment potential in vivo of human progenitor T cells generated from hematopoietic stem cells. *Blood.* 2009 Jul 30; 114 (5) :972-82. PubMed PMID:19491395.

8. Schiefner A, Wilson IA. Presentation of lipid antigens by CD1 glycoproteins. *Curr Pharm Des.* 2009; 15 (28) :3311-7. PubMed PMID:19860680; PubMed Central PMCID: PMC3096567.

9. Zlotoff DA, Schwarz BA, Bhandoola A. The long road to the thymus: the generation, mobilization, and circulation of T-cell progenitors in mouse and man. *Semin Immunopathol.* 2008 Dec; 30 (4) :371-82. PubMed PMID:18925398.

10. Rothenberg EV, Scripture-Adams DD. Competition and collaboration: *Gata-3*, PU1, and Notch signaling in early T-cell fate determination. *Semin Immunol.* 2008 Aug; 20 (4) :236-46. PubMed PMID:18768329; PubMed Central PMCID: PMC2634812.

11. Kamath MB, Houston IB, Janovski AJ, Zhu X, Gowrisankar S, Jegga AG, DeKoter RP. Dose-dependent repression of T-cell and natural killer cell genes by PU1 enforces myeloid and B-cell identity. *Leukemia.* 2008 Jun; 22 (6) :1214-25. PubMed PMID:18354487.

12. Hao QL, George AA, Zhu J, Barsky L, Zielinska E, Wang X, Price M, Ge S, Crooks GM. Human intrathymic lineage commitment is marked by differential CD7 expression: identification of CD7- lympho-myeloid thymic progenitors. *Blood.* 2008 Feb 1; 111 (3) :1318-26. PubMed PMID:17959857; PubMed Central PMCID: PMC2214748.

13 Schmittgen TD, Livak KJ. Analyzing real-time PCR data by the comparative C(T) method. *Nat Protoc.* 2008; 3 (6) :1101-8. PubMed PMID:18546601.

14. Awong G, La Motte-Mohs RN, Zúñiga-Pflücker JC. In vitro human T cell development directed by notch-ligand interactions. *Methods Mol Biol.* 2008; 430:135-42. PubMed PMID:18370296.

15. Six EM, Bonhomme D, Monteiro M, Beldjord K, Jurkowska M, Cordier-Garcia C, Garrigue A, Dal Cortivo L, Rocha B, Fischer A, Cavazzana-Calvo M, André-Schmutz I. A human postnatal lymphoid progenitor capable of circulating and seeding the thymus. *J Exp Med.* 2007 Dec 24; 204 (13) :3085-93. PubMed PMID:18070935; PubMed Central PMCID: PMC2150974.

16. Bjorklund A, Aschan J, Labopin M, Remberger M, Ringden O, Winiarski J, Ljungman P. Risk factors for fatal infectious complications developing late after allogeneic stem cell transplantation. *Bone Marrow Transplant.* 2007 Dec; 40 (11) :1055-62. PubMed PMID:17891187.

17. Eapen M, Logan BR, Confer DL, Haagenson M, Wagner JE, Weisdorf DJ, Wingard JR, Rowley SD, Stroncek D, Gee AP, Horowitz MM, Anasetti C. Peripheral blood grafts from unrelated donors are associated with increased acute and chronic graft-versus-host disease without improved survival. *Biol Blood Marrow Transplant.* 2007 Dec; 13 (12) :1461-8. PubMed PMID:18022576; PubMed Central PMCID: PMC2267869.

18. Nervi B, Rettig MP, Ritchey JK, Wang HL, Bauer G, Walker J, Bonyhadi ML, Berenson RJ, Prior JL, Piwnica-Worms D, Nolta JA, DiPersio JF. Factors affecting human T cell engraftment, trafficking, and associated xenogeneic graft-

vs-host disease in NOD/SCID beta2mnull mice. *Exp Hematol.* 2007 Dec; 35 (12) :1823-38. PubMed PMID:17764813; PubMed Central PMCID: PMC2238776.

19. Friedman AD. Transcriptional control of granulocyte and monocyte development. *Oncogene*. 2007 Oct 15; 26 (47) :6816-28. PubMed PMID:17934488.

20. Poutsiaka DD, Price LL, Ucuzian A, Chan GW, Miller KB, Snydman DR. Blood stream infection after hematopoietic stem cell transplantation is associated with increased mortality. *Bone Marrow Transplant*. 2007 Jul; 40 (1) :63-70. PubMed PMID:17468772.

21. Weerkamp F, Baert MR, Brugman MH, Dik WA, de Haas EF, Visser TP, de Groot CJ, Wagemaker G, van Dongen JJ, Staal FJ. Human thymus contains multipotent progenitors with T/B lymphoid, myeloid, and erythroid lineage potential. *Blood*. 2006 Apr 15; 107 (8) :3131-7. PubMed PMID:16384926.

22. Haddad R, Guimiot F, Six E, Jourquin F, Setterblad N, Kahn E, Yagello M, Schiffer C, Andre-Schmutz I, Cavazzana-Calvo M, Gluckman JC, Delezoide AL, Pflumio F, Canque B. Dynamics of thymus-colonizing cells during human development. *Immunity*. 2006 Feb; 24 (2) :217-30. PubMed PMID:16473833.

23. García-Ojeda ME, Dejbakhsh-Jones S, Chatterjea-Matthes D, Mukhopadhyay A, BitMansour A, Weissman IL, Brown JM, Strober S. Stepwise development of committed progenitors in the bone marrow that generate functional T cells in the absence of the thymus. *J Immunol*. 2005 Oct 1; 175 (7) :4363-73. PubMed PMID:16177077.

24. Israel E, Kapelushnik J, Yermiahu T, Levi I, Yaniv I, Shpilberg O, Shubinsky G. Expression of CD24 on CD19- CD79a+ early B-cell progenitors in human bone

marrow. *Cell Immunol*. 2005 Jul-Aug; 236 (1-2) :171-8. PubMed PMID:16181617.

25. Dik WA, Pike-Overzet K, Weerkamp F, de Ridder D, de Haas EF, Baert MR, van der Spek P, Koster EE, Reinders MJ, van Dongen JJ, Langerak AW, Staal FJ. New insights on human T cell development by quantitative T cell receptor gene rearrangement studies and gene expression profiling. *J Exp Med.* 2005 Jun 6; 201 (11) :1715-23. PubMed PMID:15928199; PubMed Central PMCID: PMC2213269.

26. Buitenhuis M, van Deutekom HW, Verhagen LP, Castor A, Jacobsen SE, Lammers JW, Koenderman L, Coffer PJ. Differential regulation of granulopoiesis by the basic helix-loop-helix transcriptional inhibitors Id1 and *Id2*. *Blood*. 2005 Jun 1; 105 (11) :4272-81. PubMed PMID:15701714.

27. Liu C, Ueno T, Kuse S, Saito F, Nitta T, Piali L, Nakano H, Kakiuchi T, Lipp M, Hollander GA, Takahama Y. The role of CCL21 in recruitment of T-precursor cells to fetal thymi. *Blood*. 2005 Jan 1; 105 (1) :31-9. PubMed PMID:15358618.

28. Haddad R, Guardiola P, Izac B, Thibault C, Radich J, Delezoide AL, Baillou C, Lemoine FM, Gluckman JC, Pflumio F, Canque B. Molecular characterization of early human T/NK and B-lymphoid progenitor cells in umbilical cord blood. *Blood.* 2004 Dec 15; 104 (13) :3918-26. PubMed PMID:15331438.

29. Benz C, Heinzel K, Bleul CC. Homing of immature thymocytes to the subcapsular microenvironment within the thymus is not an absolute requirement for T cell development. *Eur J Immunol*. 2004 Dec; 34 (12) :3652-63. PubMed PMID:15484191.

30. De Smedt M, Hoebeke I, Plum J. Human bone marrow CD34+ progenitor cells mature to T cells on OP9-DL1 stromal cell line without thymus microenvironment. *Blood Cells Mol Dis*. 2004 Nov-Dec; 33 (3) :227-32. PubMed PMID:15528136.

31. Witt CM, Robey EA. The ins and outs of CCR7 in the thymus. *J Exp Med*. 2004 Aug 16; 200 (4) :405-9. PubMed PMID:15314071; PubMed Central PMCID: PMC2211929.

32. Busslinger M. Transcriptional control of early B cell development. *Annu Rev Immunol.* 2004; 22:55-79. PubMed PMID:15032574.

33. Klein F, Feldhahn N, Lee S, Wang H, Ciuffi F, von Elstermann M, Toribio ML, Sauer H, Wartenberg M, Barath VS, Krönke M, Wernet P, Rowley JD, Müschen M. T lymphoid differentiation in human bone marrow. *Proc Natl Acad Sci U S A*. 2003 May 27; 100 (11) :6747-52. PubMed PMID:12738882; PubMed Central PMCID: PMC164518.

34. Rossi MI, Yokota T, Medina KL, Garrett KP, Comp PC, Schipul AH Jr, Kincade PW. B lymphopoiesis is active throughout human life, but there are developmental age-related changes. *Blood*. 2003 Jan 15; 101 (2) :576-84. PubMed PMID:12393702.

35. Schmitt TM, Zúñiga-Pflücker JC. Induction of T cell development from hematopoietic progenitor cells by delta-like-1 in vitro. *Immunity*. 2002 Dec; 17 (6) :749-56. PubMed PMID:12479821.

36. Rothenberg EV. T-lineage specification and commitment: a gene regulation perspective. *Semin Immunol.* 2002 Dec; 14 (6) :431-40. PubMed PMID:12457616.

37. Sabek O, Dorak MT, Kotb M, Gaber AO, Gaber L. Quantitative detection of T-cell activation markers by real-time PCR in renal transplant rejection and correlation with histopathologic evaluation. *Transplantation*. 2002 Sep 15; 74 (5) :701-7. PubMed PMID:12352889.

38. Friedman AD. Transcriptional regulation of granulocyte and monocyte development. *Oncogene*. 2002 May 13; 21 (21) :3377-90. PubMed PMID:12032776.

39. de Yébenes VG, Carrasco YR, Ramiro AR, Toribio ML. Identification of a myeloid intrathymic pathway of dendritic cell development marked by expression of the granulocyte macrophage-colony-stimulating factor receptor. *Blood*. 2002 Apr 15; 99 (8) :2948-56. PubMed PMID:11929786.

40. Maury S, Mary JY, Rabian C, Schwarzinger M, Toubert A, Scieux C, Carmagnat M, Esperou H, Ribaud P, Devergie A, Guardiola P, Vexiau P, Charron D, Gluckman E, Socié G. Prolonged immune deficiency following allogeneic stem cell transplantation: risk factors and complications in adult patients. *Br J Haematol*. 2001 Dec; 115 (3) :630-41. PubMed PMID:11736948.

41. Dejbakhsh-Jones S, Garcia-Ojeda ME, Chatterjea-Matthes D, Zeng D, Strober S. Clonable progenitors committed to the T lymphocyte lineage in the mouse bone marrow; use of an extrathymic pathway. *Proc Natl Acad Sci U S A*. 2001 Jun 19;

98 (13) :7455-60. PubMed PMID:11390986; PubMed Central PMCID: PMC34690.

42. Ikawa T, Fujimoto S, Kawamoto H, Katsura Y, Yokota Y. Commitment to natural killer cells requires the helix-loop-helix inhibitor *Id2*. *Proc Natl Acad Sci U S A*. 2001 Apr 24; 98 (9) :5164-9. PubMed PMID:11296270; PubMed Central PMCID: PMC33181.

43. Dejbakhsh-Jones S, Strober S. Identification of an early T cell progenitor for a pathway of T cell maturation in the bone marrow. *Proc Natl Acad Sci U S A*. 1999 Dec 7; 96 (25) :14493-8. PubMed PMID:10588733; PubMed Central PMCID: PMC24464.

44. Youn BS, Kim CH, Smith FO, Broxmeyer HE. TECK, an efficacious chemoattractant for human thymocytes, uses GPR-9-6/CCR9 as a specific receptor. *Blood*. 1999 Oct 1; 94 (7) :2533-6. PubMed PMID:10498628.

45. Hendriks RW, Nawijn MC, Engel JD, van Doorninck H, Grosveld F, Karis A. Expression of the transcription factor *Gata-3* is required for the development of the earliest T cell progenitors and correlates with stages of cellular proliferation in the thymus. *Eur J Immunol*. 1999 Jun; 29 (6) :1912-8. PubMed PMID:10382753.

46. Dalloul AH, Patry C, Salamero J, Canque B, Grassi F, Schmitt C. Functional and phenotypic analysis of thymic CD34+CD1a- progenitor-derived dendritic cells: predominance of CD1a+ differentiation pathway. *J Immunol*. 1999 May 15; 162 (10) :5821-8. PubMed PMID:10229816.

47. Plum J, De Smedt M, Verhasselt B, Offner F, Kerre T, Vanhecke D, Leclercq G, Vandekerckhove B. In vitro intrathymic differentiation kinetics of human fetal

liver CD34+CD38- progenitors reveals a phenotypically defined dendritic/T-NK precursor split. *J Immunol*. 1999 Jan 1; 162 (1) :60-8. PubMed PMID:9886370.

48. Puel A, Ziegler SF, Buckley RH, Leonard WJ. Defective IL7R expression in T(-)B(+)NK(+) severe combined immunodeficiency. *Nat Genet*. 1998 Dec; 20 (4) :394-7. PubMed PMID:9843216.

49. Gary-Gouy H, Lang V, Sarun S, Boumsell L, Bismuth G. In vivo association of CD5 with tyrosine-phosphorylated ZAP-70 and p21 phospho-zeta molecules in human CD3+ thymocytes. *J Immunol*. 1997 Oct 15; 159 (8) :3739-47. PubMed PMID:9378960.

50. Plum J, De Smedt M, Leclercq G, Verhasselt B, Vandekerckhove B. Interleukin-7 is a critical growth factor in early human T-cell development. *Blood*. 1996 Dec 1; 88 (11) :4239-45. PubMed PMID:8943859.

51. Cheng T, Shen H, Giokas D, Gere J, Tenen DG, Scadden DT. Temporal mapping of gene expression levels during the differentiation of individual primary hematopoietic cells. *Proc Natl Acad Sci U S A*. 1996 Nov 12; 93 (23) :13158-63. PubMed PMID:8917561; PubMed Central PMCID: PMC24063.

52. Ishiguro A, Spirin KS, Shiohara M, Tobler A, Gombart AF, Israel MA, Norton JD, Koeffler HP. *Id2* expression increases with differentiation of human myeloid cells. *Blood*. 1996 Jun 15; 87 (12) :5225-31. PubMed PMID:8652837.

53. Res P, Martínez-Cáceres E, Cristina Jaleco A, Staal F, Noteboom E, Weijer K, Spits H. CD34+CD38dim cells in the human thymus can differentiate into T, natural killer, and dendritic cells but are distinct from pluripotent stem cells. *Blood*. 1996 Jun 15; 87 (12) :5196-206. PubMed PMID:8652833.

54. Ktorza S, Blanc C, Laurent C, Sarun S, Verpilleux MP, Debré P, Schmitt C. Complete TCR-delta rearrangements and partial (D-J) recombination of the TCR-beta locus in CD34+7+ precursors from human cord blood. *J Immunol*. 1996 Jun 1; 156 (11) :4120-7. PubMed PMID:8666778.

55. Galy A, Travis M, Cen D, Chen B. Human T, B, natural killer, and dendritic cells arise from a common bone marrow progenitor cell subset. *Immunity*. 1995 Oct; 3 (4) :459-73. PubMed PMID:7584137.

56. Spits H, Lanier LL, Phillips JH. Development of human T and natural killer cells. *Blood*. 1995 May 15; 85 (10) :2654-70. PubMed PMID:7742523.

57. Galy AH, Cen D, Travis M, Chen S, Chen BP. Delineation of T-progenitor cell activity within the CD34+ compartment of adult bone marrow. *Blood*. 1995 May 15; 85 (10) :2770-8. PubMed PMID:7537981.

58. Schmitt C, Ktorza S, Sarun S, Verpilleux MP, Blanc C, Deugnier MA, Dalloul A, Debré P. CD34-positive early stages of human T-cell differentiation. *Leuk Lymphoma*. 1995 Mar; 17 (1-2) :43-50. PubMed PMID:7539659.

59. Raab M, Yamamoto M, Rudd CE. The T-cell antigen CD5 acts as a receptor and substrate for the protein-tyrosine kinase p56lck. *Mol Cell Biol*. 1994 May; 14 (5) :2862-70. PubMed PMID:7513045; PubMed Central PMCID: PMC358654.

60. Schmitt C, Ktorza S, Sarun S, Blanc C, De Jong R, Debre P. CD34-expressing human thymocyte precursors proliferate in response to interleukin-7 but have lost myeloid differentiation potential. *Blood*. 1993 Dec 15; 82 (12) :3675-85. PubMed PMID:7505122.

61. Yeoman H, Gress RE, Bare CV, Leary AG, Boyse EA, Bard J, Shultz LD, Harris DT, DeLuca D. Human bone marrow and umbilical cord blood cells generate CD4+ and CD8+ single-positive T cells in murine fetal thymus organ culture. *Proc Natl Acad Sci U S A*. 1993 Nov 15; 90 (22) :10778-82. PubMed PMID:7902570; PubMed Central PMCID: PMC47861.

62. Galy A, Verma S, Bárcena A, Spits H. Precursors of CD3+CD4+CD8+ cells in the human thymus are defined by expression of CD34 Delineation of early events in human thymic development. *J Exp Med*. 1993 Aug 1; 178 (2) :391-401. PubMed PMID:7688021; PubMed Central PMCID: PMC2191105.

63. Chabannon C, Wood P, Torok-Storb B. Expression of CD7 on normal human myeloid progenitors. *J Immunol*. 1992 Sep 15; 149 (6) :2110-3. PubMed PMID:1381397.

64. Terstappen LW, Huang S, Picker LJ. Flow cytometric assessment of human T-cell differentiation in thymus and bone marrow. *Blood*. 1992 Feb 1; 79 (3) :666-77. PubMed PMID:1370641.

65. Marine J, Winoto A. The human enhancer-binding protein Gata3 binds to several T-cell receptor regulatory elements. *Proc Natl Acad Sci U S A*. 1991 Aug 15; 88 (16) :7284-8. PubMed PMID:1871134; PubMed Central PMCID: PMC52279.

66. Schanberg LE, Fleenor DE, Kurtzberg J, Haynes BF, Kaufman RE. Isolation and characterization of the genomic human CD7 gene: structural similarity with the murine Thy-1 gene. *Proc Natl Acad Sci U S A*. 1991 Jan 15; 88 (2) :603-7. PubMed PMID:1703303; PubMed Central PMCID: PMC50860.

67. Maraninchi D, Gluckman E, Blaise D, Guyotat D, Rio B, Pico JL, Leblond V, Michallet M, Dreyfus F, Ifrah N. Impact of T-cell depletion on outcome of allogeneic bone-marrow transplantation for standard-risk leukaemias. *Lancet*. 1987 Jul 25; 2 (8552) :175-8. PubMed PMID:2885638.

68. Civin CI, Strauss LC, Brovall C, Fackler MJ, Schwartz JF, Shaper JH. Antigenic analysis of hematopoiesis III A hematopoietic progenitor cell surface antigen defined by a monoclonal antibody raised against KG-1a cells. *J Immunol*. 1984 Jul; 133 (1) :157-65. PubMed PMID:6586833.

69. Dik WA, Pike-Overzet K, Weerkamp F, de Ridder D, de Haas EF, Baert MR, van der Spek P, Koster EE, Reinders MJ, van Dongen JJ, Langerak AW, Staal FJ. New insights on human T cell development by quantitative T cell receptor gene rearrangement studies and gene expression profiling. J Exp Med. 2005 Jun 6; 201 (11) :1715-23. PubMed PMID:15928199; PubMed Central PMCID: PMC2213269.

70. Blom B, Spits H. Development of human lymphoid cells. Annu Rev Immunol. 2006; 24:287-320. PubMed PMID:16551251.

71. Rothenberg EV. T cell lineage commitment: identity and renunciation. J Immunol. 2011 Jun 15; 186 (12) :6649-55. PubMed PMID:21646301; PubMed Central PMCID: PMC3111953.

72. Awong G, La Motte-Mohs RN, Zúñiga-Pflücker JC. In vitro human T cell development directed by notch-ligand interactions. Methods Mol Biol. 2008; 430:135-42. PubMed PMID:18370296.